# *Reviews*

## Semiconductor-Based Composite Materials: Preparation, Properties, and Performance

Krishnan Rajeshwar,* Norma R. de Tacconi, and C. R. Chenthamarakshan

*Department of Chemistry and Biochemistry, The University of Texas at Arlington, Arlington, Texas 76019-0065*

*Received March 19, 2001. Revised Manuscript Received May 24, 2001*

A diverse array of semiconductor-based composite materials have been prepared, characterized, and utilized in many applications ranging from photocatalysis, photovoltaic cells, photoelectrochromic displays, and light-emitting devices to sensors. The composite architectures (nanoarchitectures in many cases) are equally diverse. In this review, we highlight the advances that have been made and identify some of the gaps in our current knowledge of these materials. Size quantization effects and semiconductor quantum dots are also discussed.

### 1. Introduction and Scope of Review

Nature has been producing remarkable composites for millions of years. Timber and bone are two examples that come to mind. They are made up of cellulose fibers in lignin and hydroxyapatite in collagen, respectively. As in other fields of scientific and technological endeavor, mankind has attempted to develop artificial analogues of these natural materials. The bricks that the ancient Egyptian civilization developed by adding straw to mud are among the earliest examples of man-made composite materials. Rubber and rubber-based composites (e.g., automobile tires) constitute more recent examples.

What is the technological driver in the quest for new composite materials? It is quite simply the desire to secure a property (or a combination of properties) not available in any of the individual components in the composite. Classically, improved strength (or other mechanical attributes) have been the characteristics sought. In more recent years, high electrical and thermal conductivities have been targeted for the composite relative to its constituents.

Within the narrower context of electrochemistry/photochemistry/photophysics and photoelectrochemistry/photocatalysis, composite films and particles have been increasingly studied and utilized in many laboratories around the world. The performance figure-of-merit of the composite in these instances is the magnitude of an electrical response (current, voltage, or their photoinduced counterparts) or an optical response (e.g., luminescent light emission). Alternately, a chemical response parameter such as reactant conversion rate or a product yield can also be used as an evaluation tool.

In this review, we will first survey preparation methods of various types of semiconductor-based composites. We will then present selected examples where these composite materials have shown enhanced performance relative to their counterparts in the "neat" state. Our discussion is confined to *semiconductor-based* composite materials. Thus, the "active component" in the materials of interest here is predominantly an inorganic compound semiconductor such as a metal oxide or metal chalcogenide.

Some of the systems discussed below fall under the category of nanocomposites in that at least one of the phase dimensions (length, width, or thickness) is in the nanometer-size range.[1] As discussed elsewhere,[1] the special properties of the nanocomposite arise from the interactions of its phases at the interfaces. While the semiconductor-based nanocomposite counterparts are no exception to this trend, size-quantized optical and optoelectronic effects bring a new dimension to their study because both the light absorption and light emission characteristics of semiconductor particles are drastically modified in the nanometer-size (and subnanometer-size) regime.[2−7]

What would be the practical incentives for studying semiconductor-based composite materials? They are attractive materials for a variety of optoelectronic applications, including light-emitting devices and optical switches. They can be used in solar photovoltaic devices and as chemical/biological sensors. Composites in the nanometer-size range that contain a magnetic component (e.g., $\gamma$-$Fe_2O_3$) ("nanomagnets") exhibit unusual phenomena and physical properties leading to diverse application areas, ranging from information storage and color imaging to medical diagnosis. Semiconductor-based composites can also be deployed in energy-storage and environmental remediation applications. Clearly,

* To whom correspondence should be addressed. E-mail: rajeshwar@uta.edu.

10.1021/cm010254z CCC: $20.00 
Published on Web 07/17/2001

**Table 1. Some Elemental and Compound Semiconductors and Their Optical Characteristics[a]**

| semiconductor | band-gap energy, eV | approximate threshold wavelength, nm |
|---|---|---|
| | Elemental | |
| Si | 1.12 | 1107 |
| Ge | 0.66 | 1879 |
| | Oxides | |
| $TiO_2$ (rutile) | 3.00 | 413 |
| (anatase) | 3.15 | 394 |
| ZnO | 3.35 | 370 |
| $WO_3$ | 3.2 | 388 |
| $MoO_3$ | 2.9 | 428 |
| $Fe_2O_3$ | 2.2 | 564 |
| $SnO_2$ | 3.8 | 326 |
| | Chalcogenides | |
| CdS | 2.42 | 512 |
| CdSe | 1.70 | 729 |
| CdTe | 1.50 | 827 |
| ZnS | 3.2 | 388 |
| ZnSe | 2.58 | 481 |
| PbS | 0.50 | 2480 |
| HgS | 0.50 | 2480 |
| HgTe | 0.14 | 8857 |
| | Groups III−V (13−15) Compounds | |
| GaAs | 1.43 | 867 |
| GaP | 2.24 | 554 |
| InAs | 0.33 | 3758 |
| InP | 1.29 | 960 |

[a] The optical parameters listed are *bulk* values; i.e., those in the absence of size-quantization (SQ) effects (see text). These data also pertain to room temperature.

the above examples illustrate the enormous range and diversity in the application possibilities for these materials. This article will examine how the optical, optoelectronic, and/or the photoelectrochemical and photocatalytic properties of a given semiconductor are enhanced by the composite architecture. As a prelude to this review, these properties of a semiconductor are briefly discussed first.

## 2. Optical, Optoelectronic, and Photoelectrochemical Properties of a Semiconductor

The optical response of a semiconductor is critically controlled by its energy band gap ($E_g$) which gives the threshold energy for an electronic transition from the valence band to the conduction band.[8] In molecular terms, such a transition would be analogous to the lowest energy electronic transition wherein an electron in the highest occupied molecular orbital (HOMO) is promoted to the lowest unoccupied molecular orbital (LUMO). Table 1 lists the values of $E_g$ and the corresponding wavelength cutoff limits for the semiconductors of interest here. As can be seen, these span a wide range of energies (and wavelengths) from ≈0.1 eV (infrared) to ≈1.5 eV (visible) and ultimately approaching the regime of insulators, that is, ≈4 eV (deep UV).

Radiative deactivation resulting from electron−hole pair recombination processes (either band-to-band or mediated by states in the gap region or at the semiconductor surface) results in light emission or luminescence. Luminescence is a powerful tool, both for characterizing the semiconductor and for constructing useful devices. We shall consider several instances below where this spectroscopic probe has furnished useful insights into the photophysical/photochemical behavior of the composite.

When electronic particles such as electrons and holes are constrained by potential barriers to regions of space that are comparable to or smaller than their de Broglie wavelength, the corresponding allowed energy states become discrete (i.e., quantized) rather than continuous. This manifests in the absorption (or emission) spectra as discrete lines that are reminiscent of atomic (line) transitions; these sharper features often appear superimposed on a broader envelope. Another manifestation for semiconductors is that $E_g$ increases or, equivalently, the absorption threshold exhibits a blue shift. The critical dimension for size quantization (SQ) effects to appear in semiconductors depends on the effective mass ($m^*$) of the electronic charge carriers. For $m^*/m_0 \sim 0.05$ ($m_0$ = free electron mass), the critical dimension is about 300 Å; it decreases approximately linearly with increasing $m^*$.[2−7] The effective mass is a measure of the total amount of mass that moves when a particular mode of motion occurs. For quantum mechanical particles such as electrons, relativistic considerations obviously apply. Further, the effective mass of an electron is determined by the second derivative (i.e., curvature) of the kinetic energy−wave vector space.

In general, charge carriers in semiconductors can be confined in one, two, or three spatial dimensions, giving rise to quantum wells, quantum wires, or quantum particles (or dots). There is much scientific and technological interest in SQ effects in semiconductors. One underlying reason is that the optical, electrical, and redox properties of semiconductors can be tuned simply by manipulating their physical dimensions rather than their chemical composition. There is also a fundamental incentive to explore how atomic and molecular properties evolve into bulk ones. Much of this body of work, particularly that stemming from electrochemical, photophysical, and photochemical perspectives, has been reviewed elsewhere.[2−7] Our focus here is on semiconductor quantum dots ("Q-dots") in *composite* matrixes.

When the semiconductor phase contacts a medium capable of undergoing charge transfer (e.g., liquid containing a redox agent), we have the interesting interplay of photophysical and electrochemical phenomena. Such "photoelectrochemical" systems have been intensely studied in recent years.[9−13] Once again, our present interest centers on composite photoelectrochemical systems that contain, in the solid phase contacting the redox medium, another component (e.g., metal or polymer) besides the key semiconductor element.

Photocatalysis comprises a subset of photoelectrochemical processes where the light energy input merely serves to accelerate the reaction rate relative to the kinetics in the dark.[14] Thus, oxidation of an organic hydrocarbon has a negligible rate on a semiconductor surface in the dark, although thermodynamically it is feasible (i.e., has a negative Gibbs free energy). Upon irradiation of the semiconductor, the photogenerated holes (especially in a high band-gap semiconductor such as $TiO_2$, Table 1) will oxidize the hydrocarbon while the photogenerated electrons will reduce $O_2$. Thus, the overall photocatalytic process can be broken down into conjugate anodic and cathodic reaction components.[15]

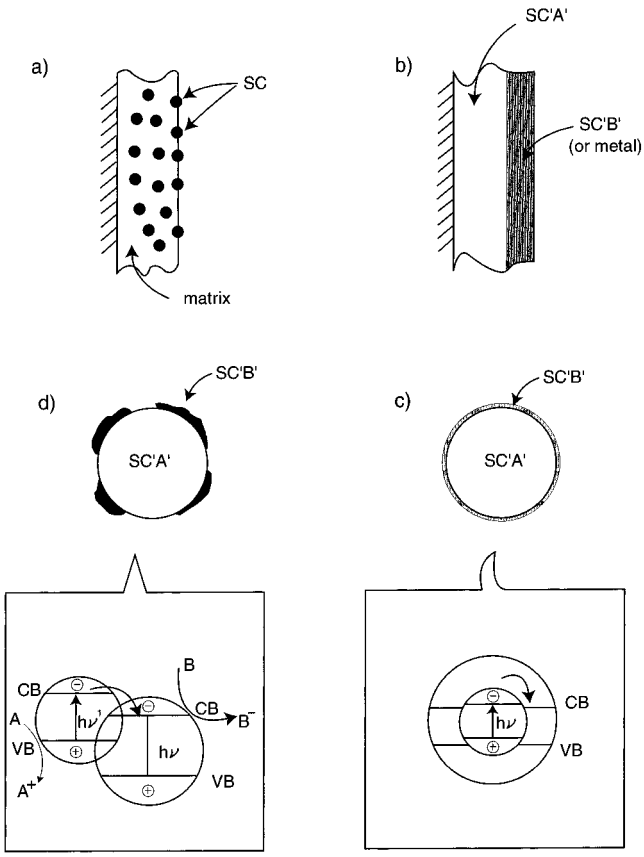


**Figure 1.** Schematic diagrams of four types of semiconductor-based composite architectures: (a) semiconductor/matrix; (b) layered configuration; (c) core−shell geometry; and (d) coupled semiconductors. The inserts in (c) and (d) schematically show the corresponding energy diagrams; "SC" denotes semiconductor.

## 3. Semiconductor-Based Composite Architectures: An Overview

The semiconductor phase comprises the key building block in the composite architectures of interest here. One or more semiconductors may be dispersed in a continuous matrix as schematized in Figure 1a. Alternately, the composite could consist of stacked layers of various components (Figure 1b). Strategies for preparing ordered arrays of semiconductor particles are also relevant to the present discussion. The use of three-dimensional crystalline superlattices (e.g., zeolites) as hosts for quantum-confined semiconductor atom arrays (such as quantum wires and Q-dots) has been reviewed by other authors.[16] We shall consider other template-based strategies for preparing semiconductor composites in what follows.

What about the semiconductor phase itself? As mentioned earlier, considerable effort has gone into preparing and characterizing size-quantized semiconductor particles and clusters as colloidal dispersions.[2−7] However, colloidal media suffer from problems associated with irreproducibility in preparation and instability. As further discussed in a subsequent section, a large body of literature exists on the use of organic or inorganic capping agents that protect the semiconductor cluster against agglomeration and other surface-related effects (see below). Frequently, the semiconductor nanoparticles (usually uncapped) are coated with another (nominally wider band gap) semiconductor in a core−shell geometry (Figure 1c). This is done for passivating the initial nanoparticle surface and enhancing its light-emissive properties as discussed later. These core−shell configurations are identified in what follows by the notation: (core) shell as exemplified by (CdSe)ZnS.

In other instances, the semiconductor may be simply physically contacted by another semiconductor particle in a "coupled" geometry (Figure 1d). Obviously, the distinction between the two configurations in Figures 1c and 1d is a matter of degree, that is, whether the second phase partially or completely engulfs the other semiconductor. An interesting aspect of composite systems, such as those depicted in Figures 1c and 1d, is that the photogenerated electrons and holes may be spatially confined in either the same particle or in different particles depending on the interfacial energetics. Alternately, the hole may be confined to the core while the electron is delocalized throughout the (core) shell structure. Such a situation has important consequences in terms of imparting enhanced photoelectrochemical stability to the system, given that many of these semiconductors (especially groups II−VI and III−V compounds) are prone to anodic photocorrosion in aqueous media.[17−19]

The two types of semiconductor nanocrystal assemblages depicted in Figures 1c and 1d are then dispersed in a suitable matrix (e.g., polymer) to afford the composite. A variety of polymers have been utilized as the matrix and examined from their functional perspective as discussed in section 4. An examination of how the matrix and the composite architecture impact the key property of the semiconductor phase (either photocurrent or light emission) constitutes a major theme of this review article. This topic is considered in section 5.

## 4. Preparative Aspects

The preceding discussion shows that a wide range of semiconductor-based composite configurations exist. Thus, it should not be surprising to note that an equally diverse array of synthetic methodologies exist for these materials as well. Space constraints prohibit a detailed discussion of each of these synthetic approaches. Instead, the key points associated with each approach are highlighted in what follows. To facilitate a focused discussion, the various synthetic strategies are reviewed within the framework of the configurations identified in the preceding discussion. Ordered arrays of semiconductor particles and Q-dot based systems are discussed separately in view of their specialized nature, and in the case of Q-dots, their distinct photophysical and photochemical behavior.

**4.1. Semiconductor−Matrix Composites.** With reference to Figure 1a, these composites comprise semiconductor particles dispersed in a host matrix that may be a metal or a polymer. Alternatively, high surface area supports such as clays, alumina, silica, or zeolites may be employed as the matrix—a tactic well-known to the heterogeneous catalysis community. Table 2 contains a summary of selected composites in this category and the corresponding synthetic route employed. We once again qualify the compilation in Table 2 (and

**Table 2. Representative Composites of the Matrix/Semiconductor Type (cf. Figure 1a) and the Corresponding Preparative Routes**

| composite[a] | preparative route | reference(s) |
|---|---|---|
| Ni/$TiO_2$ | electrodeposition | 20 |
| Ni/CdS | electrodeposition | 21 |
| Pt/$TiO_2$ | electrodeposition | 22 |
| Zn/$TiO_2$ | electrodeposition | 23 |
| polypyrrole/$TiO_2$ | electrodeposition | 24,25 |
| phthalocyanine/ZnO | electrodeposition | 26 |
| polypyrrole/$\gamma$-$Fe_2O_3$ | electrodeposition | 27 |
| phthalocyanine/$TiO_2$ | chemical | 28 |
| polyaniline/$\gamma$-$Fe_2O_3$ | chemical | 29 |
| Nafion/CdS | chemical | 30a,b |
| Nafion/ZnS | chemical | 30b |
| polypyrrole/$SnO_2$ | chemical | 31 |
| Nafion/$TiO_2$ | chemical | 32a |
| clay/$TiO_2$ | chemical | 32b,c |
| clay/$Fe_2O_3$ | chemical | 32b,33 |
| activated carbon/$TiO_2$ | chemical | 32c,34 |
| alumina/$TiO_2$ | chemical | 34,35,36b |
| silica/$TiO_2$ | chemical | 34−37 |
| zeolite/$TiO_2$ | chemical | 34,38 |
| zirconia/$TiO_2$ | chemical | 37 |
| glass microbubble/$TiO_2$ | thermolytic | 39a,b |
| fly ash/$TiO_2$ | thermolytic | 39c |
| alumina/$TiO_2$ | MOCVD | 40 |

[a] The composite is designated in each case by the matrix first followed by the dispersed semiconductor phase.

**Table 3. Representative Composites of the Layered Type (cf. Figure 1b) and the Corresponding Preparative Route**

| entry | composite[a,b] | preparative route | reference(s) |
|---|---|---|---|
| 1 | SAM/$TiO_2$ | self-assembly | 65 |
| 2 | SAM/PbS | self-assembly | 66,67 |
| 3 | $SnO_2$/$TiO_2$ | sol−gel | 68 |
| 4 | $SiO_2$/$TiO_2$ | sol−gel | 69 |
| 5 | $TiO_2$/$SiO_2$ | photo-oxidation | 70 |
| 6 | NiO/$TiO_2$ | photo-oxidation | 71 |
| 7 | $SnO_2$/ZnO | spray deposition | 72 |
| 8 | $SiO_2$/$WO_3$ | controlled hydrolysis | 73 |
| 9 | CdS/HgS | electrodeposition | 74 |
| 10 | CuSCN/polypyrrole | electrodeposition | 75 |
| 11 | $TiO_2$/$Ni(OH)_2$ | electrodeposition | 76 |
| 12 | $TiO_2$/$WO_3$ | wet impregnation | 77 |
| 13 | CoS/Ti/CdSe | electrodeposition/ slurry painting | 78 |
| 14 | GaAs/$TiO_2$ | MOCVD | 79 |
| 15 | $MoS_2$/polypyrrole | chemical polymerization | 80 |
| 16 | CuPc/$TiO_2$ | thermal evaporation | 81 |
| 17 | $TiO_2$/$MgO_x$ | adsorption/oxidation | 82 |
| 18 | $TiO_2$/Au | adsorption | 83 |
| 19 | Ag/$TiO_2$ | chemical reduction/ controlled hydrolysis | 84 |
| 20 | $TiO_2$/CdSe | colloid deposition/ electrodeposition | 85 |
| 21 | $SnO_2$/CdSe | colloid deposition/ electrodeposition | 86 |
| 22 | $SnO_2$/$TiO_2$ | colloid deposition | 87 |

[a] SAM = self-assembled monolayer; CuPc = copper phthalocyanine. [b] In the vast majority of cases, the first phase shown in the sequence constitutes the "inner" layer (i.e., atop the substrate) and the second, the "outer" layer.

others that follow in this review article) as being representative rather than exhaustive.

The preparative routes that appear in Table 2 may be broadly categorized into electrosynthetic, chemical, or thermolytic and/or gas-phase methods such as metal−organic chemical vapor deposition (MOCVD). Each of these categories is briefly discussed next.

Electrosynthetic methods for preparing semiconductor thin films have the virtues of simplicity, cost, and amenability to process control.[41−44] These syntheses are also carried out at temperatures close to ambient (unlike their high-vacuum counterparts such as CVD or molecular beam epitaxy), thus avoiding complications from preferential evaporation, zone intermixing, and so forth. The methodology for chalcogenide and oxide compound semiconductors is particularly well-developed, as reviewed elsewhere.[42−46]

The first seven composites listed in Table 2 were prepared by occlusion electrodeposition or particle codeposition.[47−52] In this technique, the matrix is electrodeposited from a precursor bath also loaded with the semiconductor particles to be occluded. Further details, including modeling aspects, have been reviewed by other authors.[48,50−52] Thus, for the composites in Table 2 containing a metal as the matrix, the corresponding ("plating") bath for (cathodic) electrodeposition of the neat metal film is used in conjunction with dosed quantities of $TiO_2$ or CdS particles in the bath.[20−23] On the other hand, the polypyrrole matrix was grown by anodic polymerization of pyrrole monomer solution[53] dosed with the $TiO_2$ particles.[24,25]

The chemical synthesis examples in Table 2 are mostly based on the sol−gel route.[54] Thus, the desired metal oxide sol is prepared by acid hydrolysis of the corresponding metal alkoxide precursor (e.g., titanium isopropoxide).[55] For mixed oxides (e.g., silica/$TiO_2$), the sols are separately prepared and then mixed to the desired composition. In the other cases, the matrix support material (e.g., clay and zeolite) is mixed with the sol with the stir time, temperature, and medium pH all being important variables. A subsequent calcination step completes the synthesis sequence. The composite growth mechanism has been studied by scanning electron microscopy (SEM), X-ray diffraction (XRD) analyses, Raman spectroscopy, energy-filtered transmission electron microscopy (EFTEM), and solid-state nuclear magnetic resonance (NMR) techniques.[38]

In addition to the synthesis approaches considered above and in Table 2, methods for depositing oxide films using high-energy techniques, such as plasma deposition,[56] sputtering,[57,58] and ion implantation,[59] have enjoyed a long and successful history, although instances for the use of them for preparing the corresponding *composite* films are relatively scarce. Similarly, the use of CVD for preparing oxide films is now rather well-established,[40,55,60−62] although variants such as pulsed beam CVD[63] will undoubtedly see wider application for composite film preparation in the future.

**4.2. Layered Composites.** In this section we consider the preparation of composites in which the semiconductor phase and the other components are organized as layers in two dimensions (cf. Figure 1b). Layer-by-layer assembly of polyelectrolyte−inorganic semiconductor "sandwich" films has been discussed by other authors.[64] The incorporation of clays after ion exchange with cationic surfactants ("clay organocomplexes") into such assemblages has also been reviewed.[64] We will avoid overlap with these earlier discussions and consider other examples of semiconductor-based layered composites in what follows below.

Table 3 contains representative systems in this category and the corresponding synthetic route employed. As with their counterparts in Table 2, an equally

(or perhaps more) diverse array of synthetic strategies has been deployed for these systems. Because of space constraints, only some salient features of the works considered in Table 3 are discussed below; the original references should be consulted for more details.

Monolayer coverage of silica on $TiO_2$ was secured by initial chemisorption of 1,3,5,7-tetramethylcyclotetrasiloxane on the titania surface.[70] The chemisorption was shown to occur via Ti−O−Si bonds by diffuse reflectance infrared Fourier transform (DRIFT) spectroscopy.[88] While these oxide particles floated in water, subsequent irradiation ($\lambda$ > 300 nm) caused them to undergo the "photosinking" phenomenon.[89] Once again the DRIFT spectral data were consistent with photooxidation of the adsorbed silane precursor to Si−OH groups on the $TiO_2$ surface. The same group employed an initial adsorption step this time by a magnesium acetylacetonate precursor followed by thermal oxidation to yield controlled amounts of $MgO_x$ on the $TiO_2$ surface.[82]

As in the earlier instances in Table 2, electrosynthesis provides a convenient method for preparing layered composites, as exemplified by entries 9, 10, and 11 in Table 3. Cuprous thiocyanate is a p-type semiconductor with a band gap of 3.6 eV.[90] A bilayer structure of CuSCN/polypyrrole has been grown by first electrodepositing polypyrrole on the Cu surface from a nonaqueous medium. This modified electrode is then repeatedly cycled in an aqueous solution of KSCN (Figure 2). Interestingly the thiocyanate anions permeate through the (microporous) polymer layer and anodically reacts with the underlying Cu surface to afford an inner layer of CuSCN.[75]

Raman spectroscopy furnishes useful insights into the bilayer architecture. Figure 3 contains two sets of in situ Raman spectra in KSCN electrolyte for the Cu/CuSCN/polypyrrole bilayer compared with an inverted glassy carbon/polypyrrole/CuSCN sequence.[75] The key difference is the absence of the higher frequency "bound" $\nu$(CN) spectral feature in the latter case. Thus, while the 2067-$cm^{-1}$ band is present in both cases (because of the KSCN electrolyte), the polypyrrole overlayer in the Cu/CuSCN/polypyrrole case prevents excitation (and/or transmission) of the signal from the underlying CuSCN layer. Interestingly, the Raman spectral data in Figure 3 also afford insights into the relative thickness of the two layers. The CuSCN layer must obviously be much thinner than the polypyrrole layer because the Raman spectral features from the polypyrrole layer are present, even in Figure 3a; that is, the CuSCN overlayer is not thick enough to completely inhibit the excitation of the (underlying) polypyrrole layer. Note, however, that the polypyrrole spectral features in Figure 3a are diminished in amplitude (relative to their counterparts in Figure 3b), attesting to some attenuation (by the CuSCN layer) of the excitation light. Thus, in situ Raman spectroscopy provides not only crucial insights into the layered morphology and film quality (i.e., an uneven top coating would have yielded signals from the underlayer) but also valuable information into relative film thicknesses in layered configurations. Other virtues of Raman spectroscopy as an in situ characterization tool have been recently espoused by other authors.[91]

CdS/HgS heterojunctions have been prepared[74] by an electrochemical variant of atomic layer epitaxy (ALE),

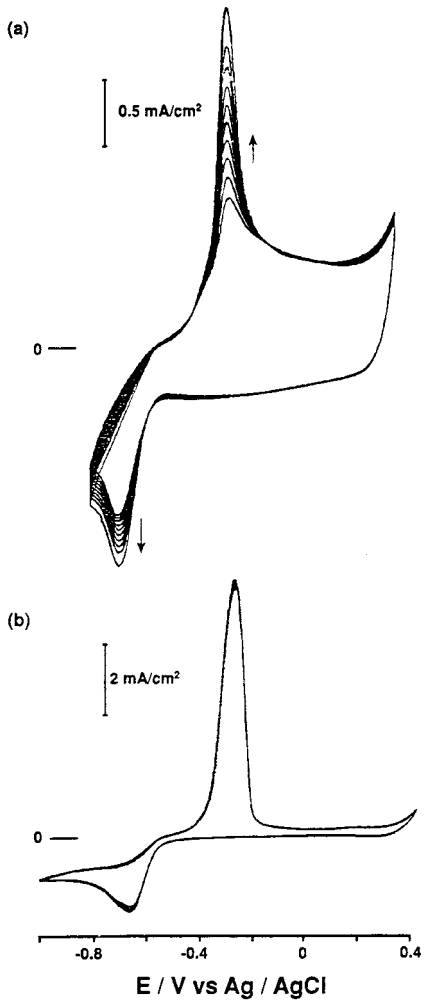


**Figure 2.** Electrosynthetic growth of a layered CuSCN/polypyrrole composite. (a) Cyclic voltammograms on repeated cycling of a Cu/polypyrrole electrode in KSCN electrolyte. (b) Corresponding voltammogram for a bare Cu electrode in KSCN signaling anodic CuSCN growth and its reduction on the return cycle. From ref 75.

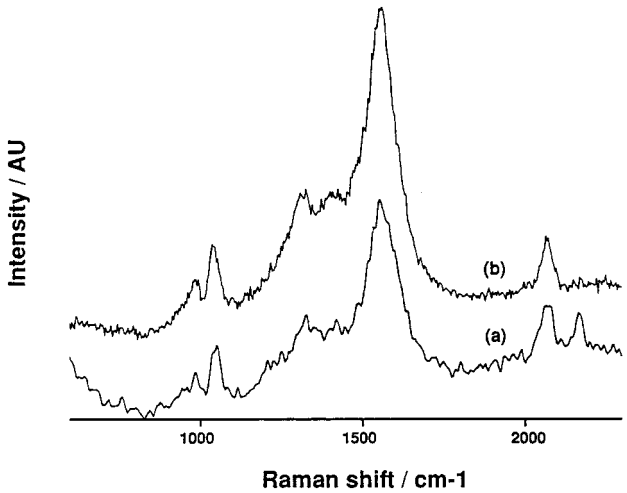


**Figure 3.** Comparison of in situ laser Raman spectra in KSCN electrolyte for (a) GC/poly-pyrrole/CuSCN and (b) Cu/CuSCN/polypyrrole composite architecture. From ref 75.

namely, ECALE.[92] The resultant architectures were characterized by scanning tunneling microscopy (STM) and photoluminescence spectroscopy. The carrier quan-

tum confinement aspects of such structures are considered later in this article. Electrosynthesis has also been employed as one of the steps in hybrid synthetic sequences as exemplified by entries 13, 20, and 21 in Table 3. Bipolar CdSe/CoS semiconductor photoelectrode panels, capable of undergoing vectorial electron transfer, were prepared[78] on titanium foils by coating one side with CdSe using slurry painting[93] and the other side with CoS using electrodeposition.

As an example of nanocomposite organic/inorganic materials, architectured at the molecular level, entry 15 contains a system where polypyrrole is intercalated into $MoS_2$. An aqueous solution of single $MoS_2$ layers and pyrrole was oxidized with $FeCl_3$.[80] What is surprising about this process (as the authors themselves point out) is the deposition of a single-phase material as opposed to a phase-separated material composed of bulk polypyrrole and restacked $MoS_2$. Instead, a new lamellar nanocomposite material made up of $MoS_2$ layers and intercalated polypyrrole chains is obtained.[80]

**4.3. Template-Directed Composite Architectures and Host−Guest Systems.** The concepts of self-assembly (mentioned earlier) and template-directed synthesis are intertwined in that a given geometry can be readily targeted for the final composite assemblage in both instances. We shall consider two template strategies in this section, namely, those based on colloidal crystals (artificial opals) and porous alumina (alumite) membranes.

Ordered arrays of polymer (e.g., polystyrene or poly(methyl methacrylate), PMMA) or silica nanospheres have been extensively studied in recent years for photonic crystal applications.[94−104] Such systems can be used as the "host" for chemically or electrochemically immobilizing semiconductor particles. Thus, the pores and voids of the ordered matrix can be filled with a metal, semiconductor, or both, which act as the "guest" material. The guest follows the symmetry layout of the voids or pores in the host matrix by self-organization, resulting in the formation of a 3-D array nanoarchitecture. Figure 4 contains two examples of the sort of order prevalent in such template architectures.[120]

Another template architecture based on porous oxide growth on aluminum under anodic bias in various electrolytes has been investigated for over 40 years.[105] Porous alumina-based templates are particularly attractive for the preparation of nanoscale composites because of their regular (and controllable) pore size distribution and interpore spacings (see Figure 5).[105−109,120] The pore density and pore diameter of the template depend on the anodizing voltage and other variables (e.g., acid used).[106g] Figure 5A illustrates a cross-sectional scanning electron micrograph of a commercial alumina (Anapore, 100-nm pore) membrane.[120] On the other hand, the alumite structure consists of hexagonal close-packed cells (Figure 5B) and details associated with the self-organization of these ordered structures in the template are being systematically elucidated.[106g,107]

Tables 4 and 5 contain examples of semiconductors deposited in these two template architectures. Thus, "microporous" $TiO_2$ films were prepared[106b] by a two-step replicating process, where PMMA was first used as a negative relief structure by growing it on the alumina template and dissolving away the latter in concentrated NaOH (Figure 6). The oxide film was then grown on the PMMA relief by sol−gel methodology and dip coating. Finally, the PMMA phase was dissolved away in acetone, leaving the $TiO_2$ film with the nanoholes in it. These nanoarchitectures were also subjected to postdeposition heat treatment.[106b] The significant aspect of this study was that the films had straight micropores of high aspect ratios and the distribution of the pore diameter was very sharp, as in the original template exemplified by Figure 5A.

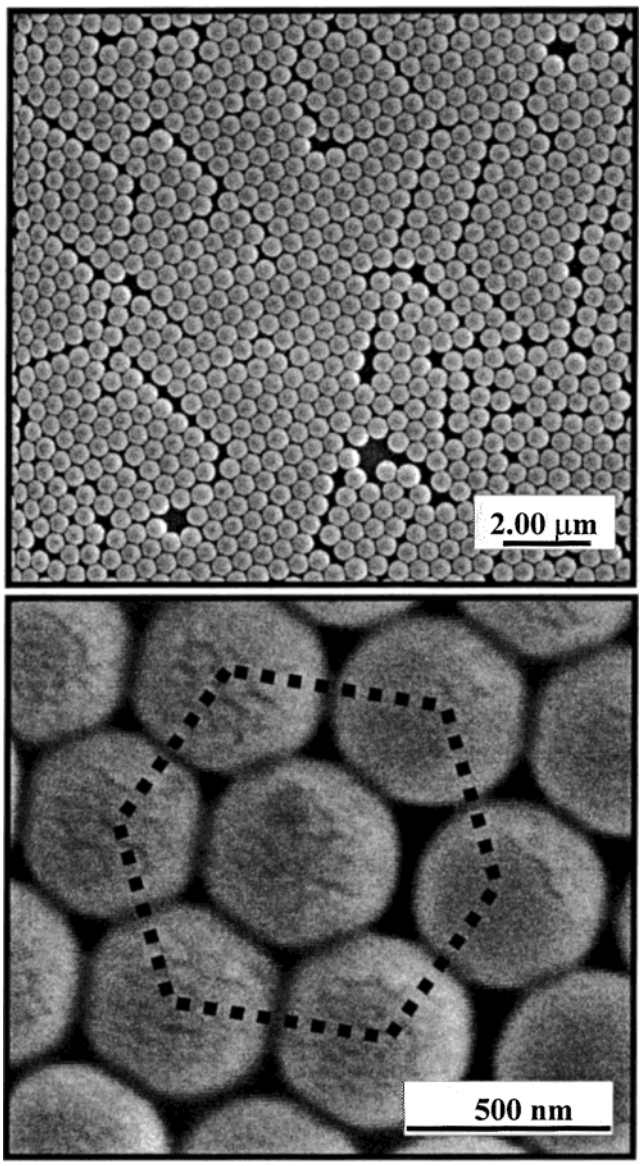


**Figure 4.** SEM micrographs of self-assembled films of silica nanospheres on a gold surface. The lower micrograph illustrates the hexagonal symmetry of the "colloidal crystal" layer. From ref 120.

In a more recent study,[114] $TiO_2$ was electrodeposited onto alumite using an ac electrolysis method. The (electro)chemical modification of the alumite template was done in two stages by these authors, as schematically shown in Figure 7. Both steps were deemed to be important by the authors, and it can be seen from Figure 7 that the second step results in the complete coverage of the alumite structure by a 6−7 $\mu$m $TiO_2$ layer. This layer was found to comprise of nanosized

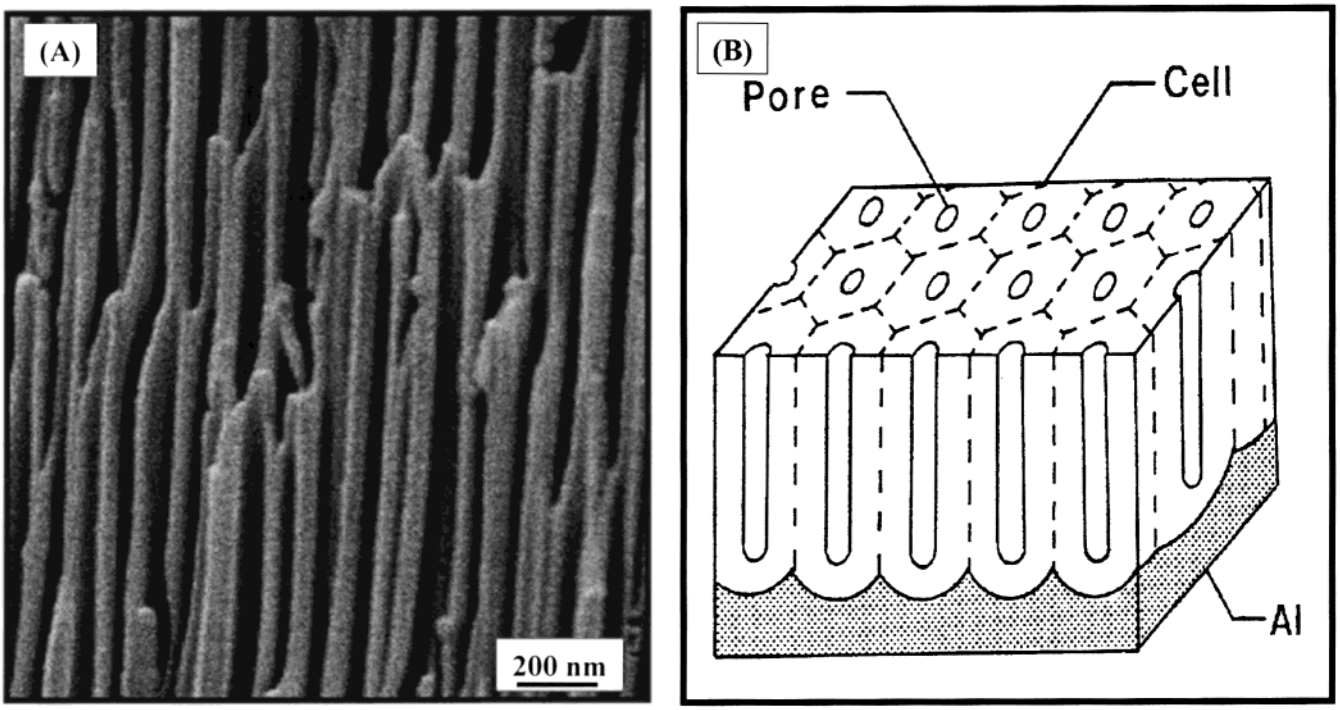


**Figure 5.** (A) Cross-sectional SEM micrograph of a 100-nm pore alumina membrane. From ref 120. (B) Schematic diagram of an alumite film. From ref 106g.

**Table 4. Examples of Semiconductors Deposited in a Silica Template Host Matrix**

| guest semiconductor(s) | deposition route | reference(s) |
|---|---|---|
| CdS | chemical (2-step) | 98b |
| CdSe | chemical (2-step) | 98b |
| CdS | CVD | 99 |
| $TiO_2$ | CVD | 98a,c |
| InP | MOCVD | 98a,c |
| $TiO_2$ | precipitation | 101 |
| CdTe | electrophoretic deposition | 110a |
| CdS | CBD | 111 |
| CdS | electrodeposition | 112 |
| CdSe | electrodeposition | 112 |
| $TiO_2$ | sol−gel | 113 |
| (CdSe)CdS[a] | colloidal | 110b |

[a] Core−shell geometry used; see ref 110b for further details.

**Table 5. Examples of Semiconductors Deposited in a Porous Alumina (Alumite) Template Host Matrix**

| guest semiconductor | deposition route | reference(s) |
|---|---|---|
| $TiO_2$ | sol−gel | 106b |
| $TiO_2$ | electrodeposition | 114 |
| $TiO_2$ | atomic layer deposition (modified atomic layer epitaxy)[115b] | 115a |
| CdSe | electrodeposition | 116 |
| CdTe | electrodeposition | 116 |
| CdS | electrodeposition | 117 |
| CdS | electrodeposition | 118 |
| CdSe | electrodeposition | 119a |
| SnS | electrodeposition | 119b |
| CuSCN | electrodeposition | 120 |
| Se | electrodeposition | 120 |

$TiO_2$ particles with anatase, rutile, and amorphous phases.

In the vast majority of case studies in Tables 4 and 5, a three-step procedure is utilized. The template is first assembled from a self-organizing system. Second, the targeted host material is grown in the voids of the template. In the third step of the process, the template is removed by calcination.[102,103] Either chemical bath deposition (CBD) or chemical vapor deposition (CVD) has been utilized for the second (growth) step. However, CdSe and CdS were grown by potentiostatic and galvanostatic deposition respectively using either polystyrene (0.466 $\mu$m diameter) or silica (1 $\mu$m diameter) spheres.[112] In both cases, three-dimensional periodic structures of the chalcogenide semiconductor were obtained after the template was removed. Electrodeposition was also employed by other authors for the alumina template for depositing CdSe.[116]

Figure 8 contains representative SEM micrographs for the anodic electrosynthesis of CuSCN in an alumite template before (Figure 8a) and after (Figure 8b) electrodeposition of CuSCN in it.[120] That the new phase is CuSCN is clearly indicated by the cyclic voltammetry signatures in Figure 9. Figure 9a contains a "normal" voltammogram for the anodic formation of CuSCN and its subsequent reduction during the return scan as obtained for a "macrosized" gold electrode containing a copper film on it.[75,121] For comparison, Figure 9b contains the voltammogram counterpart for the nanoarchitecture derived from the alumina template. The overall shapes in the two cases are quite comparable. Further, the facts that the currents are an order-of-magnitude lower and the voltammogram in Figure 9b has a more drawn-out nature are readily rationalizable by the much lower electrode area and the greater (series) resistance of the p-Si support relative to the Au support in Figure 9a.

Matrixes other than silica and alumite can be used as the host in template-derived structures.[122] The use of zeolites for this purpose was reviewed by previous authors as mentioned in an earlier paragraph.[16] Self-assembled monolayers (SAMs) based on thiolated $\beta$-cyclodextrin have been shown to be effective for securing ordered arrays of a variety of guest systems, including

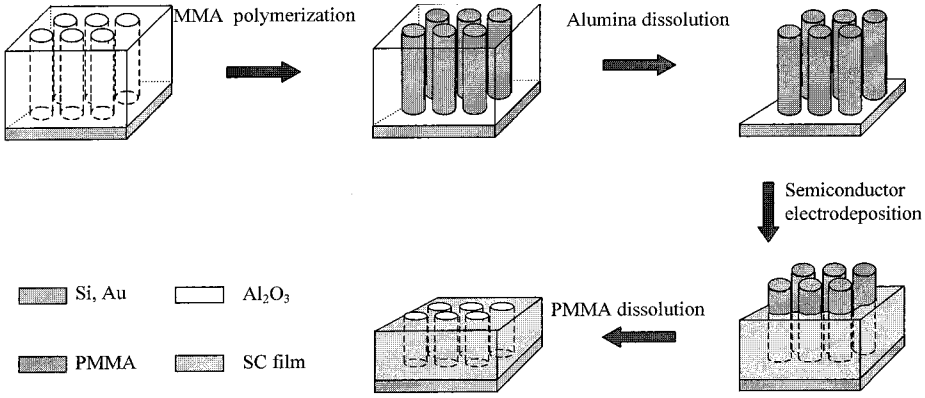


**Figure 6.** Schematic diagram for the fabrication of a $TiO_2$ film with an ordered array of nanosized holes in it.

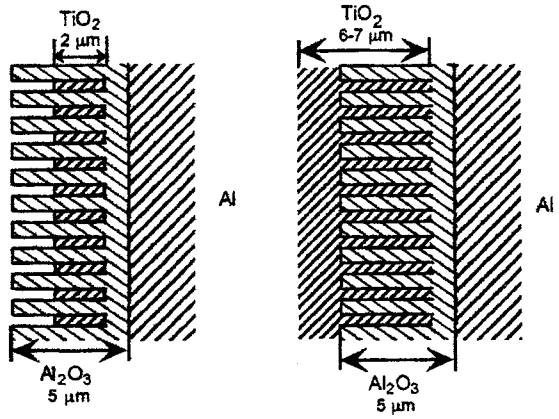


**Figure 7.** Two-stage deposition of $TiO_2$ on an alumite template resulting in the coverage and morphology schematically shown in left and right frames, respectively. From ref 114.

semiconductors.[123] Other examples for the use of SAMs or supramolecular assemblies as the host are available.[124,125] Calixarenes, which are methylene-linked phenolic macrocycles available in a number of cavity sizes,[126] have been used as the host for CdS clusters.[127] The carrier quantum-confinement (SQ) aspects of these and other systems (including those in Tables 4 and 5) are the subject of a subsequent section. Finally, even porous silicon[128] has been used as a host matrix for incorporating CdS; a sequential CBD technique was utilized for this purpose.[129] Similarly, Ge QD arrays were grown in patterned $SiO_2$ wells by a CVD process.[130]

**4.4. Quantum-Dot-Based Composites.** Bare semiconductor surfaces (even reconstructed ones) are highly reactive, and such crystallites tend to spontaneously fuse. Bare surfaces also have localized surface states, usually at energies lower than $E_g$; that is, they lie in the gap region. Thus, these intrinsic surface states contribute to electron−hole recombination, drastically reducing the luminescent quantum yield, and they also obscure size-dependent photophysical properties. Such problems are overcome with surface molecular derivatization (capping).[3b,131] A variety of capping agents have been deployed, including sodium hexametaphosphate,[132] thiols,[131,133−135] phenols,[136] thiophenols,[134,137,138] phosphines,[139] organic (phenyl) selenides,[140] and polyvinyl pyrrolidine.[141]

The precipitation of inorganic chalcogenides can be arrested kinetically at a size near the smallest homogeneous nucleation seed by employing either very high dilution and/or low temperature.[140] Improved size control (i.e., monodispersity) and colloid stability can also be secured by performing the "arrested precipitation" in structured matrixes such as inverse micelles,[131,142−144] porous glass,[5,143b] or zeolites.[5,16,145] The combination of a matrix and a "kinetic trapping agent"[134] thus imparts the desired morphological attributes to the synthesized semiconductor nanoparticles or Q-dots.

A second synthetic alternative to precipitation utilizes controlled thermolysis of organometallic precursors. By injection of these into a hot coordinating solvent such as trioctyl phosphine (TOP) and trioctyl phosphine oxide (TOPO), temporally discrete nucleation and controlled growth of capped nanocrystallites are achieved.[139] These preparations are subsequently re-dispersed in organic solvents and subjected to size-selective precipitation to achieve narrow size distributions,[146] as exemplified by the set of absorption spectra for CdSe in Figure 10.[139a] Organometallic precursors have also been used for the size-selective synthesis of groups III−V (13−15) semiconductors such as InP.[147]

More recently, the above solution growth technique has been combined with electrospray and metal−organic chemical vapor deposition (MOCVD).[148] Thus, the nanocrystals of selected size synthesized as above are dispersed in an acetonitrile/pyridine mixture and transferred into the growth zone of a MOCVD reactor using electrospray injection,[149] as a prelude to preparing more complex composite structures (see below).

Two other materials synthesis developments enhance the application possibilities of inorganic semiconductor QDs even further: namely, the use of *inorganic* capping agents leading to a (core) shell composite configuration (see Figure 1c), and the combination of a polymer matrix with the semiconductor QDs. Each of these topics is now briefly discussed.

As also discussed by other authors,[150] it is generally difficult to simultaneously passivate both anionic and cationic surface sites on a given semiconductor surface by organic ligands (i.e., organic capping agents). As a consequence, there will always be residual dangling bonds on the surface, often with deleterious electronic and photophysical consequences. On the other hand, inorganic epitaxial growth on the parent semiconductor QD surface can potentially eliminate this difficulty. A variety of such (core) shell composites have been prepared as exemplified by the compilation in Table 6.

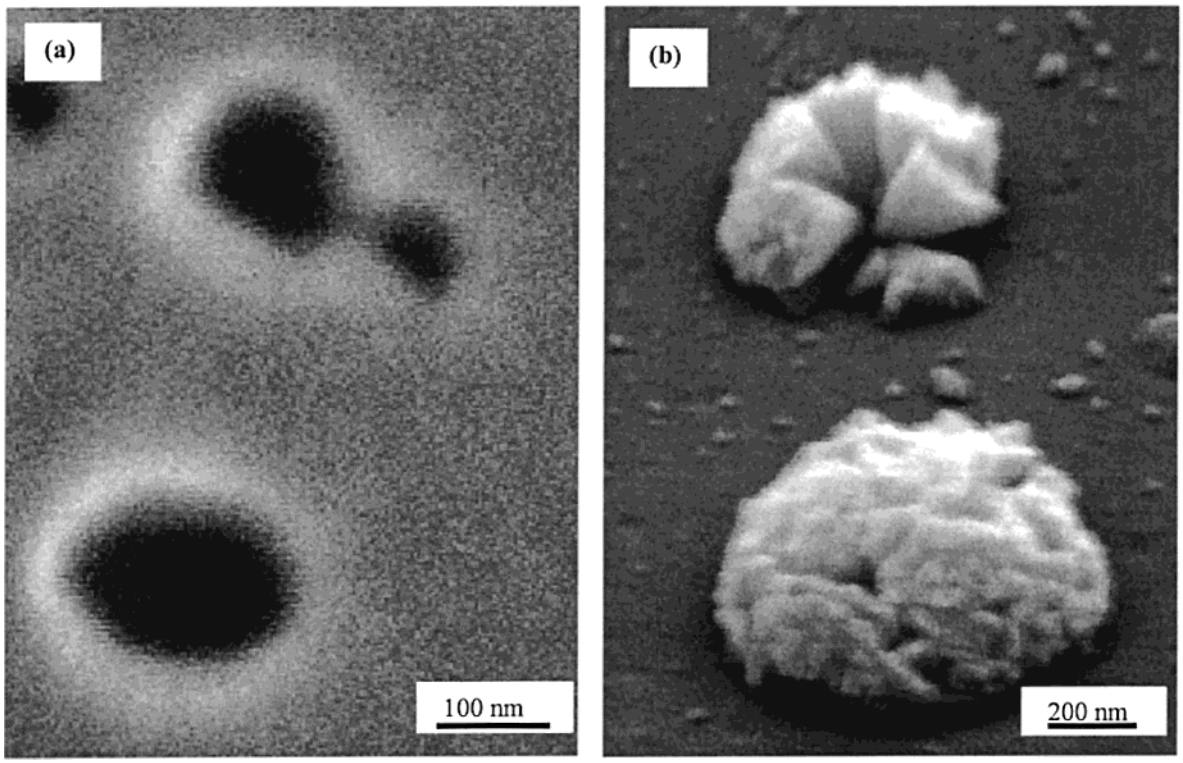


**Figure 8.** Comparison of SEM micrographs before (a) and after (b) filling of the pores in an anodized alumina thin film template with p-CuSCN. The template was supported on a p-Si wafer (see text). From ref 120.

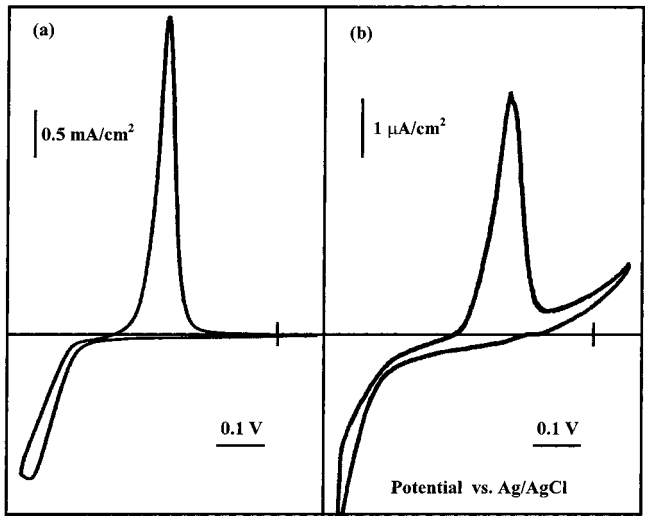


**Figure 9.** Cyclic voltammograms for the anodic growth and reduction of a p-CuSCN grown on a polycrystalline Au surface (a) and on an anodic alumina thin film template on silicon (b). Note the vastly different current scales in the two cases (see text). From ref 120.

What is the evidence for the formation of a (core) shell configuration? Recall that this type of composite is differentiated from its counterpart in Figure 1d in which the second (coupled) semiconductor only *partially* envelops the parent semiconductor surface. We must also consider the possible formation of coprecipitated crystallites of the two semiconductors or even the ternary phase.[150,156] Early work[152] used the relative attenuation of the primary photoelectron and X-ray excited Auger signals arising from the shell material to demonstrate a uniform (core) shell morphology. Shell growth was shown to be uniform and epitaxial by the use of XPS, XRD, and HRTEM for (CdSe)CdS by other authors.[150] Another diagnostic is the red shift in absorption energy that occurs with increasing shell thickness;[150,154a] this has also been modeled using effective mass theory.[154a] An interesting atom-exchange mechanism has been proposed for the (CdTe)CdS system[156] where an initial CdS "core" undergoes rapid chalcogen exchange, converting it to the ultimate CdTe core.

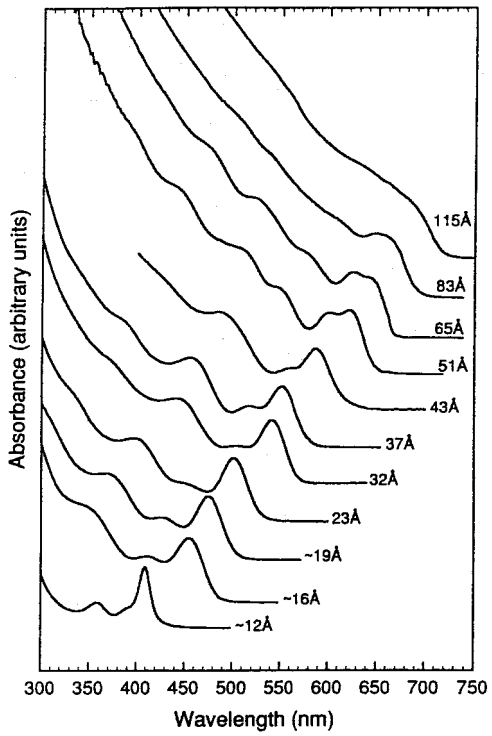


**Figure 10.** Room-temperature optical absorption spectra of CdSe nanocrystallites re-dispersed in hexane. From ref 139a.

**Table 6. Examples of Semiconductor Quantum Dot Composites of the (Core) Shell[a] Type**

| (core) shell | preparative route | reference(s) |
|---|---|---|
| (CdSe)ZnS | chemical solution growth in inverse micelles | 151 |
| (ZnS)CdSe | chemical solution growth in inverse micelles | 151 |
| (CdSe)ZnSe | chemical solution growth in inverse micelles | 152 |
| (ZnSe)CdSe | chemical solution growth in inverse micelles | 152 |
| (CdSe)ZnS | injection of organometal precursors in hot solvent | 153,154a |
| (CdSe)ZnSe | above method combined with electrospray | 154b,c |
| (CdSe)ZnS | above method combined with electrospray | 154d |
| (CdSe)CdS | injection of organometal precursors in hot solvent | 150 |
| (InP)$ZnCdSe_2$ | injection of organometal precursors in hot solvent | 155 |
| (CdTe)CdS | organometallic colloidal synthesis | 156 |
| (Ge) silane | chemical solution growth | 157 |
| (Ge) silica | chemical solution growth | 157 |
| (Si) silica | pyrolysis/oxidation | 158 |
| (CdS)HgS[b] | colloidal solution growth | 159a |
| (CdS)PbS | chemical solution growth | 160 |
| (CdS)S | hybrid electrochemical solution growth | 161 |
| $(TiO_2)MoO_3$ | modified sol−gel | 162 |

[a] The core semiconductor is identified within parentheses. See also section 3 in text. [b] Three-layered (e.g., CdS/HgS/CdS) quantum dot quantum well structures have also been prepared; see refs 159b and 159c.

Interestingly, polymeric matrixes were mainly employed, early on in the evolution of this field, for stabilization of the synthesized nanoclusters, that is, to prevent their agglomeration. More recently, attention has been paid to the functional attributes of polymeric matrixes, particularly as they relate to charge transport and passivation characteristics. Thus, Table 7 illustrates that a variety of polymers can be utilized. Such semiconductor QDs/polymer nanocomposites have been prepared by an equally diverse array of synthetic routes, ranging from simple dispersion to more elaborate schemes involving either polymerization of nanocluster functionalities[166] or ring-opening metathesis polymerization (ROMP) of suitable precursors.[170] Interestingly, in the latter cases, the polymeric matrix has a dual function in which the charge transport capability is supplemented by its passivating properties. Recall that the use of a polymeric capping agent was mentioned earlier in this section.[141]

Ion exchange and adsorption are two other routes for mating the semiconductor QDs to a polymeric backbone.[181] This principle has been extended to layer-by-layer assembly of oppositely charged polyelectrolytes (see also section 4.2 above) as exemplified by the CdTe (or HgTe)/poly(diallyl dimethylammonium chloride) (PDDA) system (entry 18) in Table 7.[180]

We close this section by noting a couple of instances of departures from the common trends in Tables 6 and 7. Thus, while compound semiconductors [particularly groups II−VI (12−16) materials] dominate the semiconductor QD literature, there are also sporadic reports of elemental semiconductor QDs, particularly those based on Si and Ge.[157,158] Second, while chemical routes dominate in the synthesis of semiconductor QDs and QD-based composites (see Tables 6 and 7), electrosynthesis (or hybrid derivatives) has also been successfully employed in attempts to secure monodispersed nanocrystals.[161,182] Size control in these cases was achieved by simultaneously employing the capping technique as an integral part of the electrosynthesis procedure.

**4.5. Summary of Synthetic Aspects.** Before proceeding to examine how the composite architecture enhances the performance of its key component, namely, the semiconductor, it is instructive to briefly pause and summarize the information presented so far in this major section. In particular, it is emphasized that the division of semiconductor-based composites into the various categories (as in Figure 1 and in sections 4.1−4.4 above) was mainly done for logistic convenience. It ought to be clear from the preceding paragraphs that there is *considerable overlap across these arbitrary boundaries*. For example, the semiconductor QD/polymer system considered in section 4.4 can be easily regarded as a subset of the semiconductor−matrix composite type discussed in section 4.1. Similarly, superlattices and quantum wells of the CdS/HgS type[159,183] can be regarded as a subset of layered composites (section 4.2). Once again, we qualify and justify the division of topics in this section by noting that it merely serves as a platform for highlighting a particular aspect of the synthesis approach.

Finally, Table 8 contains a potpourri of case studies on other semiconductor/semiconductor composites of either the (core) shell (Figure 1c) or the coupled geometry (Figure 1d). In the former case, the compilation in Table 8 is differentiated from its counterpart in Table 6 in that either the SQ effect was not directly addressed or the capping layer (on the core) was too thick to facilitate the SQ phenomenon. Other examples of coupled semiconductor composites (not explicitly considered earlier) are also included in this compilation. An earlier review by another author[202] also contains related information on these types of composites. As with the examples presented earlier, chemical and colloidal solution growth procedures were employed for preparing the vast majority of the samples in Table 8. Photocatalysis using irradiated $TiO_2$ was shown to be a simple and versatile route to the preparation of MSe (M = Pb, Cd)/$TiO_2$ composites.[197] Thus, selenium was initially deposited on $TiO_2$ particle surfaces via the photocatalytic reduction of Se(IV) species. Subsequent irradiation of these $TiO_2$/Se particles in aqueous media containing $M^{2+}$ ions resulted in MSe/$TiO_2$ growth. The mechanistic aspects of this "underpotential photocatalytic deposition" route, however, remain to be elucidated.

## 5. Illustrative Examples of Performance or Property Enhancement Induced by the Composite Architecture

In this section we present examples of performance enhancement as exhibited by semiconductor particles when they are incorporated in composite matrixes. Because of space constraints, we have to be selective in our choice of case studies.

**5.1. Photocatalysis.** As discussed earlier in section 2, band-gap irradiation of the semiconductor produces electron−hole pairs, a fraction of which (depending on the quantum yield) can be utilized in driving photo-

**Table 7. Examples of Semiconductor Quantum Dot/Polymer Nanocomposites**

| entry | polymer matrix | embedded semiconductor(s) | reference(s) |
|---|---|---|---|
| 1 | *N*-poly(vinylcarbazole) (PVK) | CdS | 163a,b |
| 2 | poly(ethylene oxide) | ZnS | 164 |
| 3 | poly (*p*-phenylene) vinylene (PPV) | CdSe | 165a,b |
| 4 | polypyridine (functionalized) | CdS | 166 |
| 5 | PVK-oxadiazole derivative | CdSe | 167 |
| 6 | poly(vinyl alcohol) | CdS | 168 |
| 7 | poly(2-methoxy,5-(2′-ethyl)-hexyloxy-PPV) (MEH−PPV) | CdSe or CdS | 169a,b,c |
| 8 | phosphine-functionalized block copolymer | CdSe or (CdSe)ZnS | 170a,b |
| 9 | polydiacetylene | CdS | 171 |
| 10 | polystyrene | Si | 172 |
| 11 | PPV | CdSe or (CdSe)ZnS | 173a,b |
| 12 | chelating polymer (Chelex) | CdS | 174 |
| 13 | polyamine dendrimer (PAMAM) | CdS | 175a,b |
| 14 | poly(3-hexylthiophene) | CdSe | 176 |
| 15 | polyacrylamide | PbS | 177 |
| 16 | polystyrene-maleic anhydride | CdS | 178 |
| 17 | poly(acrylic acid) or poly(methyl methacrylate) | ZnS (modified with Mn) | 179 |
| 18 | poly(diallyldimethylammonium chloride) | CdTe or HgTe | 180a,b |
| 19 | poly(lauryl methacrylate) | CdS or CdSe (capped with ZnS) | 154e |
| 20 | polypyrrole | CdTe | 180c |

**Table 8. Other Examples of Semiconductor/ Semiconductor Composites**

| semiconductors[a] | reference(s) | semiconductors[a] | reference(s) |
|---|---|---|---|
| $CdS/TiO_2$ | 184−188 | CdS/AgI | 186 |
| CdS/ZnO | 185a,189 | CdS/CdSe | 195 |
| $Cd_3P_2/TiO_2$ | 190a | ZnS/CdS | 196 |
| $Cd_3P_2$/ZnO | 190a | $TiO_2$/CdSe | 197 |
| $AgI/Ag_2S$ | 190b | $TiO_2$/PbSe | 197 |
| $Ag_2S$/CdS | 190c | $TiO_2/Fe_2O_3$ | 198 |
| $PbS/TiO_2$ | 191 | $LiO/TiO_2$ | 199 |
| $WO_3/WS_2$ | 192 | $WO_3/TiO_2$ | 200 |
| ZnS/ZnO | 193 | $ZnO/TiO_2$ | 201 |
| ZnSe/ZnO | 194 | | |

[a] No distinction between the (core) shell and coupled geometries is made in this compilation.

catalytic oxidation or reduction processes. Table 9 contains a selection of studies reporting an enhancement of the semiconductor photocatalytic activity in a composite configuration. There is a burgeoning body of evidence attesting to the positive influence of the matrix on the semiconductor photocatalytic activity. However, the mechanistic factors in these performance enhancements are not completely unraveled yet (see below). Factors such as electrostatics,[33,70] surface mobility,[32c,34a,36a] absorption constant of the substrate on support (matrix),[20,34a] sintering temperature/catalyst morphology,[37] and so forth have all been considered. It is even possible that no single mechanism accounts for all the observations on these composite photocatalysts!

The issue of surface mobility and energetics is an interesting one given the multiplicity of site configurations on a composite surface. We have proposed a site proximity model (Figure 11) to account for the enhancements seen for a variety of substrates and for two $TiO_2$-based composites.[20−22] The idea is that the metal sites provide the adsorption function and the (adjacent) $TiO_2$ sites serve to photoconvert the sequestered (and thus *concentrated*) substrate molecules (or ions) at the interface. Indeed, recent works have tested the premise of a positive correlation between photoinduced charge carrier separation distance and the photocatalytic activity.[206] An extension of a "Russell-like" mechanism for oxidative degradation of organic molecules was proposed by one set of authors.[206a] Thus, the photogenerated carriers ($e^-$ and $h^+$) initiate the formation of interacting chemical intermediates, that is, $O_2^{\bullet-}$ and $HOCH_2(OO)^\bullet$ (with $CH_3OH$ as the initial substrate) in *close proximity* on the catalyst surface. This mechanism eliminates the need for surface diffusion over large distances for the reaction to proceed toward the observed $CH_3COOH$ product.[206a]

Other types of effects of the *local environment* have been noted. For example, overcoating of a $TiO_2$ photocatalyst with a chlorinated silicone was found to result in an enhancement of $O_2$ uptake per photon and an altered product distribution.[39b] This was attributed to chloride ion exclusion from the reaction zone. It must be noted that while performance enhancement is the dominant trend (see Table 9), we are aware of at least two documented instances where *lower* activity was observed.[32a,b] In both these cases, $TiO_2$ particles in Nafion showed lower activity for decarboxylation of acetic acid. This lowered activity was attributed to adsorption of the Nafion sulfonate groups on the active sites of the photocatalyst.[32a,b]

**5.2. Charge Transfer, Rectification, and Photoelectrolysis.** Improved charge separation certainly is one key factor in the improvements discussed in the preceding section for many of the composites in Table 9. Single-component semiconductor nanoclusters exhibit relatively poor photocatalytic activity since the majority of the photogenerated $e^-$−$h^+$ pairs simply undergo recombination. Thus, charge rectification is a key mechanism facilitating improved quantum yields in both semiconductor−matrix (Figure 1a) and coupled semiconductor (Figure 1b) geometries. Rapid electron injection from one semiconductor to another in the coupled geometry has been either surmised from photochemical or photophysical observations[185a,190a] or directly probed by flash photolysis.[186] Interfacial electron transfer in the $TiO_2/SnO_2$ bilayer system was demonstrated to be efficient by labeling and visualizing the reduction sites with Ag particles.[68a,c]

Rectification was also demonstrated in coupled $TiO_2$/CdSe[85] and $SnO_2$/CdSe[86] films by using redox probes such as $[Fe(CN)_6]^{3-/4-}$ and cyclic voltammetry. Vectorial charge transport is the key underlying the use of coupled semiconductors for photoelectrolytic water split-

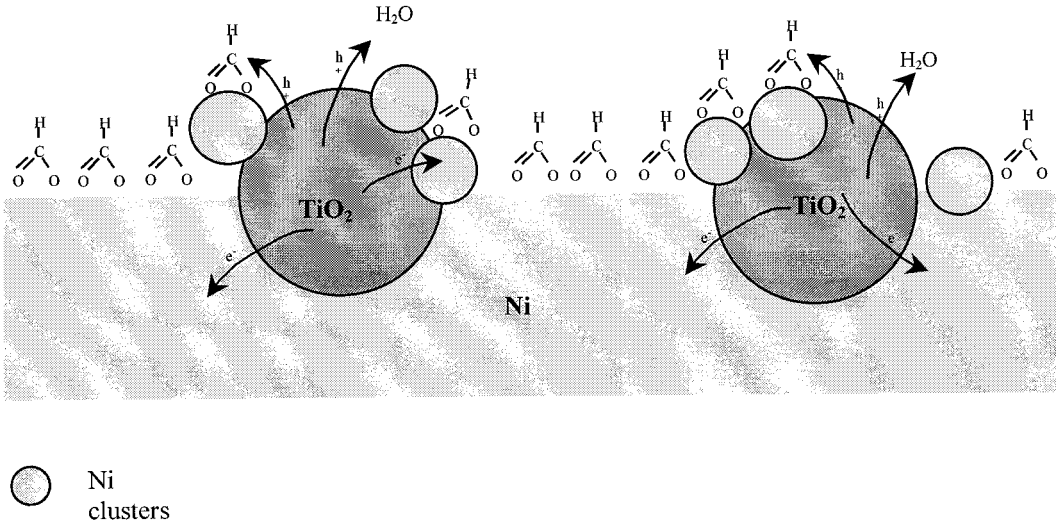


**Figure 11.** Schematic diagram of the site proximity model for a Ni/$TiO_2$ composite film with formate as a representative substrate. From refs 20c and 20d.

**Table 9. Examples of Photocatalytic Activity Enhancement in a Composite Configuration**

| composite | substrate(s) | comments | reference(s) |
|---|---|---|---|
| $\alpha$-$Fe_2O_3$/clay | acetic acid, propionic acid, *n*-butyric acid | activities dependent on solution pH | 33 |
| $SnO_2/TiO_2$ | Acid Orange 7 (azo dye) | electrochemically assisted photocatalysis | 87a |
| $SnO_2/TiO_2$ | naphthol blue black | electrochemically assisted photocatalysis | 87b |
| $TiO_2$/silica | rhodamine-6G | a ratio of $TiO_2$:$SiO_2$ of 3:7 produces maximal activity | 36a |
| $TiO_2$/zeolites | propionaldehyde | | 34a |
| $TiO_2$/alumina | propionaldehyde | | 34a |
| $TiO_2$/silica | propionaldehyde | | 34a |
| $TiO_2$/activated carbon | propionaldehyde | | 34a |
| $TiO_2$/silica | ethylene | optimum silica content was 16% (wt) | 37 |
| $TiO_2$/zirconia | ethylene | optimum zirconia content was 12% (wt) | 37 |
| $TiO_2$/activated carbon | propionaldehyde, propyzamide, bromofuran | | 32c |
| $TiO_2$/Ni | formate | enhancement correlated with composite morphology | 20 |
| CdS/Ni | sulfite | enhancement correlated with composite morphology | 21 |
| $TiO_2$/Ni | sulfite | enhancement correlated with composite morphology | 20e |
| $TiO_2$/Pt | methanol | | 22 |
| $TiO_2$/Zn | acetaldehyde | first-order rate constant increased by ~2.7 | 23 |
| $TiO_2/SiO_2$ | cetylpyridinium bromide | monolayer coverage of silica studied | 70a |
| $TiO_2/SiO_2$ | rhodamine-6G | monolayer coverage of silica studied | 70b |
| $TiO_2/MgO_x$ | sodium dodecyl-benzene sulfonate | submonolayer coverage of MgO studied | 82 |
| $TiO_2/SnO_2$ | acetaldehyde | patterning effect shown | 68b |
| $TiO_2$/Au | thiocyanate | | 203 |
| ZnSe/ZnO | thiocyanate | | 194 |
| $TiO_2$/zeolites | 4-chlorophenol, acetophenone | | 38a,b |
| $TiO_2$/Zn | acetaldehyde | activity of $TiO_2$/ZnO greater by a factor of ~1.5 | 204a |
| $TiO_2$/Ag | bis(2-dipyridyl) disulfide | enhanced activity attributed to Ag−S interaction | 204b |
| $TiO_2$/polypyrrole (or polyaniline) | 2-propanol, Fe(III) | photocatalytic electron and proton pumping demonstrated | 205 |

ting and a variety of such p−n junctions have been considered.[199,207] Other composite systems involving chalcogenide semiconductors have been deployed for photogeneration of $H_2$.[30,78,187,188] These latter case studies have practical significance in terms of solar energy storage possibilities. Some of the layered composites identified in Table 3 (e.g., CuSCN/polypyrrole, ref 75) have also been constructed with vectorial charge transport in mind.

We close this section by noting that contrasting with the considerable evidence accumulating for rapid interfacial electron transfer (on illumination) across many semiconductor/semiconductor contacts (and rectification leading to vectorial electron transfer), such evidence for semiconductor/matrix composite counterparts are currently scarce. However, data of this type have very recently appeared for Au/$TiO_2$ contacts[83,203] and more will undoubtedly appear in the future as these compos-

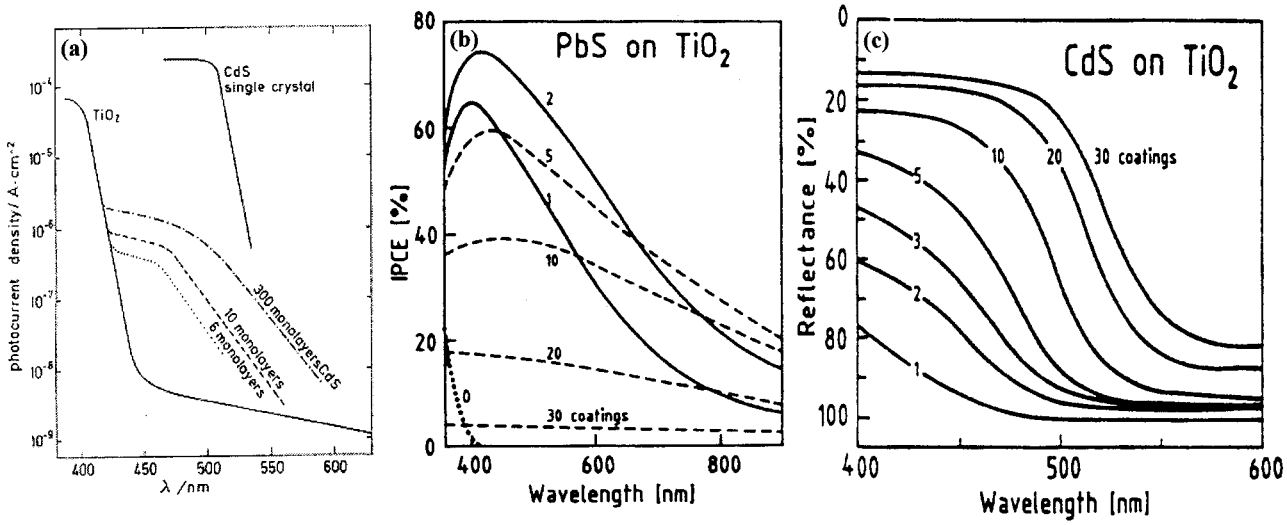


**Figure 12.** Examples of sensitization of $TiO_2$ to the visible spectral range. Photocurrent spectra (a and b) and diffuse reflectance spectra (c) of $TiO_2$ electrodes coated with CdS or PbS. From refs 184 and 217a.

ites gain widespread use and acceptance. The importance of semiconductor and metal parameters (such as the work function)[20d,208,209] is also not yet clear given that the interfaces are considerably modified from their counterparts in an ultrahigh vacuum environment.[210] Finally, the electrostatics across the composite film/solution interface and how they impact electrical parameters such as the open-circuit voltage require further scrutiny. This aspect was studied on metal-modified semiconductor *single-crystal* surfaces fairly early on in the evolution of the photoelectrochemistry field.[211] More recently, scaling factors in nanosized Schottky contacts have been addressed.[212,213]

**5.3. Spectral Sensitization and Photovoltaic Behavior.** A crucial practical difficulty with the use of $TiO_2$ for solar photovoltaic, photocatalytic, or photoelectrolytic applications is optical in nature in that its band-gap energy (3.2 eV) lies well outside the most intense region of the solar spectrum (centered at ~2.6 eV). To this end, $MoO_3$-modified $TiO_2$ core composites [$(TiO_2)$-$MoO_3$] show an interesting red shift in their photoresponse.[162] The photoabsorption energy required to promote $TiO_2$ valence band electrons to $MoO_3$ conduction band states systematically shifted from 2.88 to 2.60 eV as the composite nanoparticle size was tuned from 80 to 40 Å.[162] The degree of chemical interaction between the $TiO_2$ core and the $MoO_3$ shell was also found to play a role in the photoresponse of the composite. These composite materials, however, showed lower efficiency than Degussa P25 for the photocatalytic oxidation of acetaldehyde.[162] Nonetheless, these oxide composites appear to be more promising than approaches to sensitize $TiO_2$, which are based on the use of metal dopants.[214−216]

Spectral sensitization of wide band-gap oxides such as $TiO_2$, ZnO, $SnO_2$, $Nb_2O_5$, and $Ta_2O_5$ by Q-sized chalcogenides (CdS, PbS, $Ag_2S$, $Sb_2S_3$, and $Bi_2S_3$) was studied by other authors.[217] Photocurrent quantum yields up to ≈80% and open-circuit voltages up to ≈1 V were attained. Selected results on the sensitization of $TiO_2$ to the visible range of the solar spectrum are contained in Figure 12.[184, 217a]

Dye-sensitized photovoltaic cells based on $TiO_2$ have been extensively studied in recent years.[218] A key step in the overall photovoltaic conversion in these devices is the efficient separation of the injected electron and the photoexcited dye molecules ($D^+$). Thus, suppression of the back reaction is crucial for securing high-incident-photon-to-electron-conversion efficiency (IPCE) in these devices. Cells made from $SnO_2$/ZnO (instead of $TiO_2$) showed higher photocurrents.[219] Preliminary data also suggested higher long-term stability for the $SnO_2$/ZnO dye-sensitized cell relative to the $TiO_2$ counterpart.[219b]

The ability to construct large-area, flexible devices has led to much interest in the use of conducting polymers in photovoltaic cells. Early work on such devices, however, yielded low IPCE values.[220,221] Efficient collection of electrons and holes requires that the neutral excited states (singlet excitons) produced by photoexcitation be separated into free charge carriers. This charge separation must be fast compared to the radiative and nonradiative decays of the singlet exciton that have time constants typically in the range 100−1000 ps.

Charge separation in conjugated polymers is enhanced at the interface with a material of higher electron affinity where it is energetically favorable for the electron to transfer into the second material. The electron affinity of CdS or CdSe nanocrystals (Q-dots) is in the 3.8−4.7 eV range, compared with conjugated polymers whose electron affinity is in the 2.5−3.0 eV range.[169a] Thus, both CdS and CdSe can be used as electron acceptors in combination with conjugated polymers. Indeed, Q-dot/conducting polymer composites offer the possibility that once the electrons and holes are spatially separated into the two composite components, each carrier has a passage to the appropriate electrode without the necessity to pass through a region of the other component. Thus, carrier recombination can be potentially minimized. Photoluminescence data on CdS (or CdSe)/MEH−PPV blends[169] have shown that excitons are efficiently dissociated at the Q-dot/polymer interface, leaving the electron in the nanocrystal and the hole on the polymer.

Another factor in the improved efficiency for charge separation is the interfacial contact area between the Q-dot and polymer composite components. Transmission electron microscopy (TEM) data,[169] again on CdSe/MEH−PPV blends, have shown evidence for phase

segregation and, therefore, a large interfacial area for charge separation to occur. For high quantum efficiencies, charge *separation* must be coupled with efficient charge *transport* of the two carrier types (electrons and holes) to the respective collector electrodes. The effect of percolation of the Q-dots in the polymer matrix has been studied.[169] The (short-circuit) quantum efficiency was found to peak at 12% at ≈90% weight loading of CdSe in the MEH−PPV matrix.[169] External IPCE levels reaching 5% have been reported for such photovoltaic devices under illumination at 514 nm.

The rather low quantum efficiency (and consequently low IPCE) in the above devices was attributed to the poor transport of electrons that were thought to become trapped at "dead ends" in the nanocrystal network. If there is impediment to electron hopping to an adjacent nanocrystal, recombination with holes in the polymer matrix will occur. This problem has been tackled by the use of elongated, rod-shaped CdSe nanocrystals.[222] Thus, the use of CdSe nanorods in a regioregular poly(3-hexylthiophene) matrix resulted in almost an order of magnitude enhancement in external IPCE values (at 4.8 W/m$^2$ irradiance) to 16%.[176] Further studies will be required to boost the short-circuit currents, fill factors, and power conversion efficiencies to levels comparable to solid-state photovoltaic devices. As mentioned earlier, the single most important technology driver for the Q-dot/polymer type of photovoltaic devices, relative to current device counterparts, is their compatibility with large-area, flexible deployment (as in tents and the like) for remote solar power generation.

**5.4. Light Emission and Nanocrystal Size Monodispersity.** There has been considerable interest in light-emitting devices (LEDs) based on polymeric materials for flat panel display applications and the like. As with the photovoltaic devices discussed in the preceding section, the motivation for the use of polymers lies with their easy processability and amenability to large and flexible panel construction via relatively simple synthetic methods. The synthetic advances reviewed earlier for the preparation of highly monodisperse semiconductor Q-dots, in turn, now facilitate unprecedented control over their several spectroscopic properties, including band-edge absorption, photoluminescence (PL), and cathodoluminescence (EL). Thus, hybrid organic/inorganic LEDs using polymer-confined semiconductor Q-dots can provide emission tunable in the visible spectrum. The polymeric component in these composites can also be tailored to provide surface passivation of the nanocrystal and charge transport into the nanoparticle core, where radiative recombination takes place.

(Core) shell nanocrystals show higher quantum yields for emission since the interface of the QDs is better passivated and deep surface trap luminescence is converted into band-edge luminescence. Thus, either ZnS[153] or ZnSe[154c] capping layers dramatically enhance the band-edge luminescence of CdSe Q-dots. Similarly, lattice-matched $ZnCdSe_2$ shells improve the core emission from InP Q-dots.[155] How the structure of the ZnS shell influences the PL properties of the core has been systematically investigated using a combination of wavelength-dispersive X-ray spectroscopy, XPS, small- and wide-angle X-ray scattering, and TEM.[154a]

The use of a polymer matrix with surface-passivating and electron transport *dual* functionalities in conjunction with capped inorganic Q-dots adds a further dimension to molecular control of the LED nanoarchitecture. A variety of such polymers, appearing in the compilation in Table 7, have been deployed for this purpose. Typically in these devices the organic polymer (e.g., PPV) layer is built next to an indium tin oxide anode and serves primarily as the hole transport layer. The inorganic (Q-dot) layer is cast on an Al electrode—the thickness of this layer playing a key role in the performance of the overall heterostructure. The EL signal is seen to originate predominantly from the Q-dot layer with a weak contribution from the polymer at higher voltages.[165,173a] However, phase segregation at low concentration of the Q-dots and nanocrystal migration to the surface in films containing (CdSe)ZnS resulted in a large PPV contribution to the EL spectra.[173b] At higher concentrations, percolation sets in, resulting in spectra dominated by semiconductor Q-dot emission. Interestingly, in composite films of Mn-doped ZnS and PAA,[179] luminescence of $Mn^{2+}$ was found to be enhanced by energy transfer from the PAA matrix to the emitter centers.

Notwithstanding the impressive progress made with color tunability via control of the Q-dot size, further studies optimizing the turn-on voltage, efficiency, and stability are needed to advance this EL device technology. Luminescence is not the only optical property that is sought with semiconductor Q-dots. The refractive index and nonlinear optical (NLO) response exhibit systematic changes with the nanocrystal size as well.[171] Optical gain enhancements undergone by QDs in 3-D photonic crystal matrixes may play an important role in low-threshold microlasers based on photonic band-gap engineering.[94]

Regardless of the device type, securing tight monodispersity in the size distribution of the semiconductor Q-dots is a key to optimization of materials characteristics. Silica can be routinely prepared with such narrow size distributions. Thus, $SiO_2$ spheres have been used as templates for $TiO_2$ film deposition.[223] A physical rather than chemical "lost-wax" strategy for forming colloids with size distributions of 5% has been reported.[224] A variety of highly monodisperse inorganic, polymeric, and (core) shell colloids and hollow colloids with controllable shell thickness were synthesized using a macroporous polymer template first prepared from a silica colloidal crystal.[224] Synthetic advances that provide inorganic chalcogenide nanocrystallites with monodispersity within the limit of atomic roughness have facilitated the self-organization of 3-D semiconductor Q-dot superlattices (colloidal crystals).[225] The size and spacing of the dots within the superlattices were shown to be controllable with near atomic precision.[225]

Typically, PL emission lines for ensembles of semiconductor Q-dots are broadened as a consequence of nanoparticle size inhomogeneity. Thus, PL is a very sensitive probe of the degree of monodispersity of the Q-dot size in a given composite. PL line widths as low as 125 meV[161b] have been reported (using a hybrid electrochemical−chemical synthesis method, ref 161) for ZnO[226a] and CdS[226b] nanocrystal assemblages on conducting graphite surfaces. Remarkably, the PL is not

quenched on these conductive surfaces for reasons not clear at present. The corresponding line width for a *single* CdS (or CdSe) nanocrystal is much smaller (for, e.g., as low as <120 $\mu$eV at 10 K).[147,226c]

**5.5. Miscellaneous Aspects of Property/Performance Enhancement.** Slurry-based photocatalysis reactors do have attractive features relative to their thin-film (immobilized) photocatalyst counterparts: namely, higher photocatalyst surface area, lower susceptibility to surface poison/passivation effects, and so forth. However, one of the challenges in the further development of this technology for remediation of water-borne pollutants is an effective means of separating the photocatalyst particles from the treated water stream and recycling them into the photoreactor.[227] A magnetic core in a colloidal $TiO_2$ photocatalyst facilitates easy recovery by magnetic force application. Thus, no downstream filtration steps are required in this approach. Disappointingly, however, titania-coated magnetite particles exhibited lower photoactivity than the single-phase $TiO_2$ counterparts.[198] Nonetheless, further work appears to be warranted on magnetite-based $TiO_2$ photocatalysts.

The issue of semiconductor stability is a critical one, notwithstanding the end objective of the composite material. In a long-term stability experiment, CdSe nanocrystals and (CdSe)CdS (core) shell composites were subjected to continuous wave laser irradiation (50 W) for ≈2 h.[150] While photooxidation of the (uncapped) CdSe surfaces resulted in the "washing out" of many of its QD optical features, the (core) shell absorption spectra showed little change. This enhanced photostability was explained by the confinement of the hole in the (core) shell structure while the photogenerated electrons were delocalized and thus accessible.[150] Enhanced *thermal* stability was also observed by other authors for ZnSe-coated CdSe[154b] and CdS-coated HgTe nanocrystals.[159e] In another scenario, polymer-capped $TiO_2$ nanoparticles were found to photostabilize organic dyes.[228] On the corresponding bare surfaces of the oxide support, these dyes undergo photodegradation under visible light irradiation.

Corrosion of construction materials such as steel represents the loss of millions of dollars in the gross national product. It was found that $TiO_2$ thin film coatings, applied by a spray pyrolysis technique, cathodically photoprotected the steel surface from corrosion.[229] Similarly, a mixed $Fe_2O_3-TiO_2$ composite film exhibited enhanced corrosion resistance relative to a neat $Fe_2O_3$ surface.[230] These mixed oxide films were prepared by a cold wall low-pressure MOCVD technique.

A layered $TiO_2/Ni(OH)_2$ structure was found to exhibit strong, reversible photochromic and electrochromic properties when either UV-irradiated at open circuit or anodically polarized, respectively.[76] Vectorial transport of the photo- or electro-generated holes in $TiO_2$ and the electrons from the adjacent $Ni(OH)_2$ layer resulted in the oxidation of $Ni(OH)_2$ to NiOOH, causing its chromic transition from clear to opaque (black).[231] It must be noted that the $NiOOH-Ni(OH)_2$ electrode itself is not photoresponsive; therefore, in an electrochromic device it must be used in conjunction with a semiconductor such as $TiO_2$. A further challenge with these devices will be to sensitize $TiO_2$ to the solar spectrum so that "smart" windows can be constructed that darken (tint) upon exposure to sunlight. Unwanted solar heat gain represents a considerable waste of electrical power required for cooling office buildings and the like in summer.

We began this review with a discussion of natural and biological composite materials, and we close it with a brief note of attempts to mimic biological composite materials such as bone, teeth, and shells. These composites all consist of a polymer matrix reinforced by an inorganic phase that *crystallizes* in the matrix. They are distinguished from synthetic composites by the high degree of organization and regularity displayed by the inorganic phase. Recent studies have aimed at directed synthesis of nanocrystals (such as CdS) within a biocomposite matrix.[232,233a] A related research direction has sought to demonstrate that combinatorial phage-display libraries can be used to evolve peptides that bind to a range of semiconductor surfaces with high specificity.[233b] Contrasting with the "top-down" fabrication approach currently practiced in the semiconductor microelectronics industry, the hope is that this directed synthesis strategy may lead to "bottom-up" fabrication approaches, leading in turn to molecular electronics devices. Finally, semiconductor Q-dot/bioconjugate assemblies have been deployed for sensor applications.[234]

## 6. Concluding Remarks

Research on the synthesis and characterization of semiconductor-based composites is an extremely active field. Several types of applications are being considered for these materials and new uses will emerge in the future. The composite architecture clearly plays a crucial role in the performance of the semiconductor active component. In the vast majority of the cases documented thus far, the composite framework enhances (dramatically in many instances) the overall performance of the semiconductor component. A consequence of the inherent diversity of these materials is the need for cross-cutting approaches and concepts that must be brought to bear for better mechanistic understanding of their performance. Indeed, in the crystal ball of the present reviewers, this field is poised for further exciting developments in the months ahead as physicists, chemists, electrical engineers, and materials scientists converge on it.

**Acknowledgment.** Research in our laboratory on semiconductor-based composites is funded, in part, by a grant from the U.S. Department of Energy, Office of Basic Energy Sciences. Gloria Madden provided valuable assistance in the preparation of this article. Two reviewers also alerted us to several references in the semiconductor Q-dot literature.

## References

(1) For example: *Chem. Eng. News* **1999**, June 7, 25.
(2) (a) Brus, L. E. *J. Phys. Chem.* **1986**, *101*, 2555. (b) Brus, L. E. *Annu. Rev. Mater. Sci.* **1989**, *19*, 471. (c) Brus, L. E. *Appl. Phys. A* **1991**, *53*, 465. (d) Nirmal, M.; Brus, L. E. *Acc. Chem. Res.* **1999**, *32*, 407.
(3) (a) Henglein, A. *Chem. Rev.* **1989**, *89*, 1861. (b) Henglein, A. *Top. Curr. Chem.* **1988**, *143*, 115.
(4) (a) Weller, H. *Angew. Chem., Intl. Ed. Engl.* **1993**, *32*, 41. (b) Weller, H. *Adv. Mater.* **1993**, *5*, 88.

(5) (a) Wang, Y.; Herron, N. *J. Phys. Chem.* **1991**, *95*, 525. (b) Wang, Y. *Acc. Chem. Res.* **1991**, *24*, 133.
(6) (a) Alivisatos, A. P. *Science* **1996**, *271*, 933. (b) Alivisatos, A. P. *J. Phys. Chem.* **1996**, *100*, 13226.
(7) Kamat, P. V., Meisel, D., Eds. *Semiconductor Nanoclusters-Physical, Chemical, and Catalytic Aspects*; Elsevier: Amsterdam, 1997.
(8) Smith, R. A. *Semiconductors*; University Press: Cambridge, 1964.
(9) Pleskov, Yu. V.; Gurevich, Yu. Ya. *Semiconductor Photoelectrochemistry*; Consultants Bureau: New York, 1986.
(10) Chandra, S. *Photoelectrochemical Solar Cells*; Gordon and Breach: New York, 1985.
(11) Sato, N. *Electrochemistry at Metal and Semiconductor Electrodes*; Elsevier: Amsterdam, 1998.
(12) Finklea, H. O., Ed. *Semiconductor Electrodes*; Elsevier: Amsterdam, 1988.
(13) Rajeshwar, K.; Ibanez, J. G. *Environmental Electrochemistry*; Academic Press: San Diego, 1997.
(14) Bard, A. J. *Science* **1980**, *207*, 139.
(15) Rajeshwar, K.; Ibanez, J. G. *J. Chem. Educ.* **1995**, *72*, 1044.
(16) Stucky, G. D.; MacDougall, J. E. *Science* **1990**, *247*, 669.
(17) Bard, A. J.; Wrighton, M. S. *J. Electrochem. Soc.* **1977**, *124*, 1706.
(18) Gerischer, H. *J. Electroanal. Chem.* **1977**, *82*, 133.
(19) Meissner, D.; Memming, R.; Kastening, B. *J. Phys. Chem.* **1988**, *92*, 3476.
(20) (a) Zhou, M.; Lin, W.-Y.; de Tacconi, N. R.; Rajeshwar, K. *J. Electroanal. Chem.* **1996**, *402*, 221. (b) Zhou, M.; de Tacconi, N. R.; Rajeshwar, K. *J. Electroanal. Chem.* **1997**, *421*, 111. (c) de Tacconi, N. R.; Wenren, H.; McChesney, D.; Rajeshwar, K. *Langmuir* **1998**, *14*, 2933. (d) de Tacconi, N. R.; Boyles, C. A.; Rajeshwar, K. *Langmuir* **2000**, *16*, 5665. (e) de Tacconi, N. R.; Mrkic, M.; Rajeshwar, K. *Langmuir* **2000**, *16*, 8426.
(21) de Tacconi, N. R.; Wenren, H.; Rajeshwar, K. *J. Electrochem. Soc.* **1997**, *144*, 3159.
(22) de Tacconi, N. R.; Carmona, J.; Rajeshwar, K., unpublished results, 1999.
(23) Ito, S.; Deguchi, T.; Imai, K.; Iwasaki, M.; Tada, H. *Electrochem. Solid State Lett.* **1999**, *2*, 440.
(24) Kawai, K.; Mihara, N.; Kuwabata, S.; Yoneyama, H. *J. Electrochem. Soc.* **1990**, *137*, 1793.
(25) Beck, F.; Dahlhaus, M.; Zahedi, N. *Electrochim. Acta* **1992**, *37*, 1265.
(26) Yoshida, T.; Tochimoto, M.; Schlettwein, D.; Wohrle, D.; Sugiura, T.; Minoura, H. *Chem. Mater.* **1999**, *11*, 2657.
(27) (a) Jarjayes, O.; Auric, P. *J. Magn. Magn. Mater.* **1994**, *138*, 115. (b) Bidan, G.; Jarijayes, O.; Fruchart, J. M.; Hannecart, E. *Adv. Mater.* **1994**, *6*, 152.
(28) Liu, W.; Wang, Y.; Gui, L.; Tang, Y. *Langmuir* **1999**, *15*, 2130.
(29) Tang, B. Z.; Geng, Y.; Lam, J. W. Y.; Li, B.; Jing, X.; Wang, X.; Wang, F.; Pakhomov, A. B.; Zhang, X. X. *Chem. Mater.* **1999**, *11*, 1581.
(30) (a) Mau, A. W.-H.; Huang, C.-B.; Kakuta, N.; Bard, A. J.; Campion, A.; Fox, M. A.; White, J. M.; Webber, S. E. *J. Am. Chem. Soc.* **1984**, *106*, 6537. (b) Kakuta, N.; Park, K. H.; Finlayson, M. F.; Ueno, A.; Bard, A. J.; Campion, A.; Fox, M. A.; Webber, S. E.; White, J. M. *J. Phys. Chem.* **1995**, *89*, 732.
(31) Maeda, S.; Armes, S. P. *Chem. Mater.* **1995**, *7*, 171.
(32) (a) Miyoshi, H.; Nippa, S.; Uchida, H.; Mori, H.; Yoneyama, H. *Bull. Chem. Soc. Jpn.* **1990**, *63*, 3380. (b) Yoneyama, H. *Res. Chem. Intermed.* **1991**, *15*, 101. (c) Yoneyama, H.; Torimoto, T. *Catal. Today* **2000**, *58*, 133.
(33) Miyoshi, H.; Mori, H.; Yoneyama, H. *Langmuir* **1991**, *7*, 503.
(34) (a) Takeda, N.; Torimoto, T.; Sampath, S.; Kuwabata, S.; Yoneyama, H. *J. Phys. Chem.* **1995**, *99*, 9986. (b) Takeda, N.; Ohtani, M.; Torimoto, T.; Kuwabata, S.; Yoneyama, H. *J. Phys. Chem. B* **1997**, *101*, 2644.
(35) Minero, C.; Catozzo, G.; Pelizzetti, E. *Langmuir* **1992**, *8*, 481.
(36) (a) Anderson, C.; Bard, A. J. *J. Phys. Chem.* **1995**, *99*, 9882. (b) Anderson, C.; Bard, A. J. *J. Phys. Chem. B* **1997**, *101*, 2611.
(37) Fu, X.; Clark, L. A.; Yang, Q.; Anderson, M. A. *Environ. Sci. Technol.* **1996**, *30*, 647.
(38) (a) Xu, Y.; Langford, C. H. *J. Phys. Chem.* **1995**, *99*, 11501. (b) Xu, Y.; Langford, C. H. *J. Phys. Chem. B* **1997**, *101*, 3115. (c) Vaisman, E.; Cook, R. L.; Langford, C. H. *J. Phys. Chem. B* **2000**, *104*, 8679.
(39) (a) Heller, A. *Acc. Chem. Res.* **1995**, *28*, 503. (b) Schwitzgebel, J.; Ekerdt, J. G.; Sunada, F.; Lindquist, S.-E.; Heller, A. *J. Phys. Chem. B* **1997**, *101*, 2621. (c) Nair, M.; Luo, Z.; Heller, A. *Ind. Eng. Chem. Res.* **1993**, *32*, 2318.
(40) Lei, L.; Chu, H. P.; Hu, X.; Yue, P.-L. *Ind. Eng. Chem. Res.* **1999**, *38*, 3381.
(41) McHardy, J., Ludwig, F., Eds. *Electrochemistry of Semiconductors and Electronics*; Noyes Publications: Park Ridge, NJ, 1992; Chapter 1, pp 1−52.
(42) Rajeshwar, K. *Adv. Mater.* **1992**, *4*, 23.
(43) Hodes, G. In *Physical Electrochemistry*; Rubinstein, I., Ed.; Marcel Dekker: New York, 1995; Chapter 11, pp 515−554.
(44) Pandey, R. K.; Sahu, S. N.; Chandra, S. *Handbook of Semiconductor Electrodeposition*; Marcel Dekker: New York, 1996.
(45) Switzer, J. A. *Am. Ceram. Soc. Bull.* **1987**, *66*, 1521.
(46) Therese, H. A. G.; Kamath, P. V. *Chem. Mater.* **2000**, *12*, 1195.
(47) Hovestad, A.; Janssen, L. J. J. *J. Appl. Electrochem.* **1995**, *40*, 519.
(48) Stojak, J. L.; Fransaer, J.; Talbot, J. B. *Adv. Electrochem. Sci. Eng.*, in press.
(49) (a) Rajeshwar, K.; de Tacconi, N. R. in ref 7, pp 321−351. (b) Rajeshwar, K.; de Tacconi, N. R. In *Interfacial Electrochemistry*; Wieckowski, A., Ed.; Marcel Dekker: New York, 1999; pp 721−736.
(50) Vereecken, P. M.; Shao, I.; Searson, P. C. *J. Electrochem. Soc.* **2000**, *147*, 2572. See also references therein.
(51) Guglielmi, N. *J. Electrochem. Soc.* **1972**, *119*, 1009.
(52) Celis, J. P.; Roos, J. R. *J. Electrochem. Soc.* **1977**, *124*, 1508.
(53) Doblhofer, K.; Rajeshwar, K. In *Handbook of Conducting Polymers*; Skotheim, T. A., Elsenbaumer, R. L., Reynolds, J. R., Eds.; Marcel Dekker: New York, 1998; pp 531−588.
(54) Brinker, C. J.; Scherer, G. W. *Sol−Gel Science*; Academic Press: New York, 1990.
(55) Taylor, C. J.; Gilmer, D. C.; Colombo, D. G.; Wilk, G. D.; Campbell, S. A.; Roberts, J.; Gladfelter, W. L. *J. Am. Chem. Soc.* **1999**, *121*, 5220.
(56) Wang, R.; Henager, C. H., Jr. *J. Electrochem. Soc.* **1979**, *126*, 83.
(57) Soliman, A. A.; Seguin, H. J. J. *Solar Energy Mater.* **1981**, *5*, 95.
(58) Weber, M. F.; Schumacher, L. C.; Dignam, M. J. *J. Electrochem. Soc.* **1982**, *129*, 2022.
(59) Yamashita, H.; Honda, M.; Harada, M.; Ichihashi, Y.; Anpo, M.; Hirao, T.; Itoh, N.; Iwamoto, N. *J. Phys. Chem. B* **1998**, *102*, 10707.
(60) Fitzgibbons, E. T.; Sladek, K. J.; Hartwig, W. H. *J. Electrochem. Soc.* **1972**, *119*, 735.
(61) Leboda, R.; Turov, V. V.; Marciniak, M.; Malygin, A. A.; Malkov, A. A. *Langmuir* **1999**, *15*, 8441.
(62) Ding, Z.; Hu, X.; Lu, G. Q.; Yue, P.-L.; Greenfield, P. F. *Langmuir*, in press.
(63) For example: Doring, H.; Hashimoto, K.; Fujishima, A. *Ber. Bunsen-Ges. Phys. Chem.* **1992**, *96*, 620.
(64) (a) Fendler, J. H.; Meldrum, F. C. *Adv. Mater.* **1995**, *7*, 607. (b) Fendler, J. H. *Chem. Mater.* **1996**, *8*, 1616.
(65) Koutmoto, K.; Seo, S.; Sugiyama, T.; Seo, W. S.; Dressik, W. J. *Chem. Mater.* **1999**, *11*, 2305.
(66) Sun, Y.; Hao, E.; Zhang, X.; Yang, B.; Gao, M.; Shen, J. *Chem. Commun.* **1996**, 2381.
(67) Ogawa, S.; Hu, K.; Fan, F.-R. F.; Bard, A. J. *J. Phys. Chem. B* **1997**, *101*, 5707.
(68) (a) Tada, H.; Hattori, A.; Tokihisa, Y.; Imai, K.; Tohge, N.; Ito, S. *J. Phys. Chem. B* **2000**, *104*, 4587. (b) Hattori, A.; Tokihisa, Y.; Tada, H.; Tohge, N.; Ito, S.; Hongo, K.; Shiratsuchi, R.; Nogami, G. *J. Sol-Gel Sci. Tech.*, in press. (c) Hattori, A.; Tokihisa, Y.; Tada, H.; Ito, S. *J. Electrochem. Soc.* **2000**, *47*, 2279.
(69) Kim, W. B.; Choi, S. H.; Lee, J. S. *J. Phys. Chem. B* **2000**, *104*, 8670.
(70) (a) Tada, H.; Kubo, Y.; Akazawa, M.; Ito, S. *Langmuir* **1998**, *14*, 2936. (b) Tada, H.; Akazawa, M.; Kubo, Y.; Ito, S. *J. Phys. Chem. B* **1998**, *102*, 6360.
(71) Uekawa, N.; Suzuki, T.; Ozeki, S.; Kaneko, K. *Langmuir* **1992**, *8*, 1.
(72) Tennakone, K.; Senadeera, G. K. R.; Perera, V. P. S.; Kottegoda, I. R. M.; De Silva, L. A. A. *Chem. Mater.* **1999**, *11*, 2474.
(73) Leland, J. K.; Bard, A. J. *Chem. Phys. Lett.* **1987**, *139*, 453.
(74) Gichuhi, A.; Boone, B. E.; Shannon, C. *Langmuir* **1999**, *15*, 763.
(75) de Tacconi, N. R.; Son, Y.; Rajeshwar, K. *J. Phys. Chem.* **1993**, *97*, 1042.
(76) Kostecki, R.; Richardson, T.; McLarnon, F. *J. Electrochem. Soc.* **1998**, *145*, 2380.
(77) Eible, S.; Gates, B. C.; Knozinger, H. *Langmuir* **2001**, *17*, 107.
(78) Smotkin, E. S.; Cervera-March, S.; Bard, A. J.; Campion, A.; Fox, M. A.; Mallouk, T.; Webber, S. E.; White, J. M. *J. Phys. Chem.* **1997**, *91*, 6.
(79) Marco de Lucas, M. C.; Fabreguette, F.; Collin, S.; Bourgeois, S. *Int. J. Inorg. Mater.* **2000**, *2*, 255.
(80) Wang, L.; Schindler, J.; Thomas, J. A.; Kannewurf, C. R.; Kanatzidis, M. G. *Chem. Mater.* **1995**, *7*, 1753.
(81) Takada, J.; Awaji, H.; Koshioka, M.; Nakashima, A.; Nevin, W. A. *Appl. Phys. Lett.* **1992**, *61*, 2184.
(82) Tada, H.; Yamamoto, M.; Ito, S. *Langmuir* **1999**, *15*, 3699.
(83) Chandrasekharan, N.; Kamat, P. V. *J. Phys. Chem. B* **2000**, *104*, 10851.
(84) Pastoriza-Santos, I.; Koktysh, D. S.; Mamedov, A. A.; Giersig, M.; Kotov, N. A.; Liz-Marzan, L. M. *Langmuir* **2000**, *16*, 2731.
(85) (a) Liu, D.; Kamat, P. V. *J. Electroanal. Chem.* **1993**, *347*, 451. (b) Liu, D.; Kamat, P. V. *J. Phys. Chem.* **1993**, *97*, 10769.
(86) Nasr, C.; Kamat, P. V.; Hotchandani, S. *J. Electroanal. Chem.* **1997**, *420*, 201.

(87) (a) Vinodgopal, K.; Kamat, P. V. *Environ. Sci. Technol.* **1995**, *29*, 841. (b) Vinodgopal, K.; Bedja, I.; Kamat, P. V. *Chem. Mater.* **1996**, *8*, 2180.
(88) Tada, H. *Langmuir* **1996**, *12*, 966.
(89) Fujishima, A.; Kato, T.; Maekawa, E.; Honda, K. *Denki Kagaku* **1986**, *54*, 153.
(90) Tennakone, K.; Pushpa, G. S. S.; Punchiewa, S.; Epa, G. *Electrochim. Acta* **1986**, *31*, 315.
(91) Weaver, M. J.; Zou, S.; Chan, M. Y. H. *Anal. Chem.* **2000**, *72*, 38A.
(92) Wade, T. L.; Sorenson, T. A.; Stickney, J. L. In *Interfacial Electrochemistry*; Wieckowski, A., Ed.; Marcel Dekker: New York, 1999; pp 757−768.
(93) Hodes, G.; Cahen, D.; Manassen, J.; David, M. *J. Electrochem. Soc.* **1980**, *127*, 2252.
(94) Soukoulis, C. M., Ed. *Photonic Bandgap Materials*; NATO ASI Ser. E; Kluwer: Dordrecht, The Netherlands, 1996; Vol. 315.
(95) Rarity, J., Weisbuch, C., Eds.; *Microcavities and Photonic Bandgaps*; Kluwer: Dordrecht, The Netherlands, 1996.
(96) Yamasaki, T.; Tsutsui, T. *Appl. Phys. Lett.* **1998**, *72*, 1957.
(97) Zakhidov, A. A.; Baughman, R. H.; Ighal, Z.; Cui, C.; Khayrullin, I.; Dantas, S. O.; Marti, J.; Radchenko, V. G. *Science* **1998**, *282*, 897.
(98) (a) Romanov, S. G.; Sotomayor-Torres, C. M. in ref 95, pp 275−282. (b) Romanov, S. G.; Fokin, A. V.; Tretijakov, V. V.; Butko, V. Y.; Alperovich, V. I.; Johnson, N. P.; Sotomayor-Torres, C. M. *J. Cryst. Growth* **1996**, *159*, 857. (c) Romanov, S. G.; Johnson, N. P.; Fokin, A. V.; Butkov, V. Y.; Yates, H. M.; Pemble, M. E.; Sotomayor-Torres, C. M. *Appl. Phys. Lett.* **1997**, *70*, 2091.
(99) Vlasov, Yu. A.; Luterova, K.; Pelant, I.; Honerlage, B.; Astratov, V. N. *Appl. Phys. Lett.* **1997**, *71*, 1616.
(100) Holland, B. T.; Blanford, C. F.; Stein, A. *Science* **1998**, *281*, 538.
(101) Wijnhaven, J. E. G. J.; Vos, W. L. *Science* **1998**, *281*, 802.
(102) Raman, N. K.; Anderson, M. T.; Brinker, C. J. *Chem. Mater.* **1996**, *8*, 1682.
(103) Mann, S.; Ozin, G. A. *Nature* **1996**, *382*, 313.
(104) Vlasov, Yu. A.; Yao, N.; Norris, D. J. *Adv. Mater.* **1999**, *11*, 165.
(105) Keller, F.; Hunter, M. S.; Robinson, D. L. *J. Electrochem. Soc.* **1953**, *100*, 411.
(106) (a) Masuda, H.; Tanaka, H.; Baba, N. *Chem. Lett.* **1990**, 621. (b) Masuda, H.; Nishio, K.; Baba, N. *Jpn. J. Appl. Phys.* **1992**, *31*, L1775. (c) Masuda, H.; Nishio, K.; Baba, N. *Thin Solid Films* **1993**, *223*, 1. (d) Masuda, H.; Misuno, T.; Baba, N.; Ohmori, T. *J. Electroanal. Chem.* **1994**, *368*, 333. (e) Masuda, H.; Fukeida, K. *Science* **1995**, *268*, 1466. (f) Masuda, H.; Yamada, H.; Satoh, M.; Asoh, H.; Nakoo, M.; Tamamura, T. *Appl. Phys. Lett.* **1997**, *71*, 2770. (g) Masuda, H.; Hasegwa, F.; Ono, S. *J. Electrochem. Soc.* **1997**, *144*, L127.
(107) Jessensky, O.; Muller, F.; Gosele, U. *Appl. Phys. Lett.* **1998**, *72*, 1173.
(108) Bao, X.; Li, F.; Metzger, R. M. *J. Appl. Phys.* **1996**, *79*, 4866.
(109) (a) Martin, C. R. *Science* **1994**, *266*, 1961. (b) Martin, C. R. *Chem. Mater.* **1996**, *8*, 1739.
(110) (a) Rogach, A. L.; Kotov, N. A.; Koktysh, D. S.; Ostrander, J. W.; Ragoisha, G. A. *Chem. Mater.* **2000**, *12*, 2721. (b) Rogach, A. L.; Nagesha, D.; Ostrander, J. W.; Giersig, M.; Kotov, N. A. *Chem. Mater.* **2000**, *12*, 2676.
(111) Blanco, A.; Lopez, C.; Mayoral, R.; Meseguer, F.; Mifsud, A.; Herrero, *J. Appl. Phys. Lett.* **1998**, *73*, 1781.
(112) Braun, P. V.; Wiltzius, P. *Nature* **1999**, *402*, 603.
(113) (a) Tatsuma, T.; Ikezawa, A.; Ohko, Y.; Miwa, T.; Matsue, T.; Fujishima, A. *Adv. Mater.* **2000**, *12*, 643. (b) Tatsuma, T.; Ikezawa, A.; Ohko, Y.; Miwa, T.; Fujishima, A. *Electrochem. Solid State Lett.* **2000**, *3*, 467.
(114) Matsumoto, Y.; Ishikawa, Y.; Nishida, M.; Ii, S. *J. Phys. Chem. B* **2000**, *104*, 4204.
(115) (a) Cameron, M. A.; Gartland, I. P.; Smith, J. A.; Diaz, S. F.; George, S. M. *Langmuir* **2000**, *16*, 7435. (b) George, S. M.; Ott, A. W.; Klaus, J. W. *J. Phys. Chem.* **1996**, *100*, 13121.
(116) Klein, J. D.; Herrick, R. D., II; Palmer, D.; Sailor, M. J.; Brumlick, C. J.; Martin, C. R. *Chem. Mater.* **1993**, *5*, 902.
(117) Routkevitch, D.; Bigimi, T.; Moskovits, M.; Xu, J. M. *J. Phys. Chem.* **1996**, *100*, 14037.
(118) Suh, J. S.; Lee, J. S. *Chem. Phys. Lett.* **1997**, *281*, 384.
(119) (a) Xu, D.; Shi, X.; Guo, G.; Gui, L.; Tang, Y. *J. Phys. Chem. B* **2000**, *104*, 5061. (b) Jiang, K.; Wang, Y.; Gui, L.; Tang, L., courtesy preprint.
(120) de Tacconi, N. R.; Rajeshwar, K., unpublished data, 2000.
(121) Son, Y.; de Tacconi, N. R.; Rajeshwar, K. *J. Electroanal. Chem.* **1993**, *345*, 135.
(122) For example: Bethell, D.; Brust, M.; Schiffrin, D. J.; Kiely, C. *J. Electroanal. Chem.* **1996**, *409*, 137.
(123) (a) Lee, J.-Y.; Park, S.-M. *J. Electrochem. Soc.* **2000**, *147*, 4189. (b) Choi, S.-J.; Woo, D.-H.; Myung, N.; Kang, H.; Park, S.-M., courtesy preprint.
(124) (a) Shin, H.; Collins, R. J.; De Guire, M. R.; Heuer, A. H.; Sukenik, C. N. *J. Mater. Res.* **1995**, *10*, 692. (b) Shin, H.; Collins, R. J.; De Guire, M. R.; Heuer, A. H.; Sukenik, C. N. *J. Mater. Res.* **1995**, *10*, 699. (c) Collins, R. J.; Shin, H.; De Guire, M. R.; Heuer, A. H.; Sukenik, C. N. *Appl. Phys. Lett.* **1996**, *69*, 860.
(125) Kobayashi, S.; Hanabusa, K.; Hamasuki, N.; Kimura, M.; Shirai, H.; Shinkai, S. *Chem. Mater.* **2000**, *12*, 1523.
(126) Review: Diamond, D.; Nolan, K. *Anal. Chem.* **2001**, *73*, 23A.
(127) Coffer, J. L.; Chandler, R. R.; Gutsche, C. D.; Alam, I.; Pinizzotto, R. F.; Yang, H. *J. Phys. Chem.* **1993**, *97*, 696.
(128) Canham, L. T. *Appl. Phys. Lett.* **1990**, *57*, 1046.
(129) Gros-Jean, M.; Herino, R.; Lincot, D. *J. Electrochem. Soc.* **1998**, *145*, 2448.
(130) Heath, J. R.; Williams, R. S.; Shiang, J. J.; Wind, S. J.; Chu, J.; D'Emic, C.; Chen, W.; Stanis, C. L.; Bucchignano, J. J. *J. Phys. Chem.* **1996**, *100*, 3144.
(131) Steigerwald, M. L.; Alivisatos, A. P.; Gibson, J. M.; Harris, T. D.; Kortan, R.; Muller, A. J.; Thayer, A. M.; Duncan, T. M.; Douglass, D. C.; Brus, L. E. *J. Am. Chem. Soc.* **1988**, *110*, 3046.
(132) Fojtik, A.; Weller, H.; Koch, U.; Henglein, A. *Ber. Bunsen-Ges. Phys. Chem.* **1984**, *88*, 969.
(133) Nosaka, Y.; Yamaguchi, K.; Miyama, H.; Hayashi, H. *Chem. Lett.* **1988**, 605.
(134) Herron, N.; Wang, Y.; Eckert, H. *J. Am. Chem. Soc.* **1990**, *112*, 1322.
(135) Swayambunathan, V.; Hayes, D.; Schmidt, K. H.; Liao, Y. X.; Meisel, D. *J. Am. Chem. Soc.* **1990**, *112*, 3831.
(136) Veinot, J. G. C.; Ginzburg, M.; Pietro, W. J. *Chem. Mater.* **1997**, *9*, 2117.
(137) (a) Dance, I. G.; Choy, A.; Scudder, M. L. *J. Am. Chem. Soc.* **1984**, *106*, 6285. (b) Lee, G.; Craig, D.; Ma, I.; Scudder, M.; Bailey, T.; Dance, I. G. *J. Am. Chem. Soc.* **1988**, *110*, 4863.
(138) Noglik, H.; Pietro, W. J. *Chem. Mater.* **1994**, *6*, 1593.
(139) (a) Murray, C. B.; Norris, D. B.; Bawendi, M. G. *J. Am. Chem. Soc.* **1993**, *115*, 8706. (b) Becerra, L.; Murray, C. B.; Griffin, R. G.; Bawendi, M. G. *J. Phys. Chem.* **1994**, *100*, 3297.
(140) Steigerwald, M. L.; Brus, L. E. *Acc. Chem. Res.* **1990**, *23*, 183. See also references therein.
(141) Leppert, V. J.; Mahamuni, S.; Kumbhojkar, N. R.; Risbud, S. H. *Mater. Sci. Eng.* **1998**, *B52*, 89.
(142) Meyer, M.; Wallberg, C.; Kurihara, K.; Fendler, J. H. *J. Chem. Soc., Chem. Commun.* **1984**, 90.
(143) (a) Lianos, P.; Thomas J. K. *Chem. Phys. Lett.* **1986**, *125*, 299. (b) Kuczynski, J. P.; Thomas, J. K. *J. Phys. Chem.* **1985**, *89*, 2720.
(144) Dannhauser, T.; O'Neil, M.; Johansson, K.; Whitten, D.; McLendon, G. *J. Phys. Chem.* **1986**, *90*, 6074.
(145) (a) Wang, Y.; Herron, N. *J. Chem. Phys.* **1987**, *91*, 257. (b) Herron, N.; Wang, Y.; Eddy, M. M.; Stucky, G. D.; Cox, D. E.; Moller, K.; Bein, T. *J. Am. Chem. Soc.* **1989**, *111*, 530.
(146) (a) Micic, O. I.; Curtis, C. L.; Jones, K. M.; Sprague, J. R.; Nozik, A. J. *J. Phys. Chem.* **1994**, *98*, 4966. (b) Micic, O. I.; Cheong, H. M.; Fu, H.; Zunger, A.; Sprague, J. R.; Mascarenhas, A.; Nozik, A. J. *J. Phys. Chem. B* **1997**, *101*, 4904. (c) Micic, O. I.; Jones, K. M.; Cahill, A.; Nozik, A. J. *J. Phys. Chem. B* **1998**, *102*, 9791.
(147) Empedocles, S. A.; Norris, D. J.; Bawendi, M. G. *Phys. Rev. Lett.* **1996**, *77*, 3873.
(148) Danek, M.; Jensen, K. F.; Murray, C. B.; Bawendi, M. G. *Appl. Phys. Lett.* **1994**, *65*, 2795.
(149) Fenn, J. B.; Mann, M.; Meng, C. K.; Wong, S. T.; Whitehouse, C. M. *Science* **1989**, *246*, 64.
(150) Peng, X.; Schlamp, M. C.; Kadavanich, A. V.; Alivisatos, A. P. *J. Am. Chem. Soc.* **1997**, *119*, 7019.
(151) Kortan, A. R.; Hull, R.; Opila, R. L.; Bawendi, M. G.; Steigerwald, M. L.; Carroll, P. J.; Brus, L. E. *J. Am. Chem. Soc.* **1990**, *112*, 1327.
(152) Hoener, C. F.; Allan, K. A.; Bard, A. J.; Campion, A.; Fox, M. A.; Mallouk, T.; Webber, S. E.; White, J. M. *J. Phys. Chem.* **1992**, *96*, 3812.
(153) Hines, M. A.; Guyot-Sionnest, P. *J. Phys. Chem.* **1996**, *100*, 468.
(154) (a) Dabbousi, B. O.; Rodriguez-Viejo, J.; Mikulec, F. V.; Heine, J. R.; Mattoussi, H.; Ober, R.; Jensen, K. F.; Bawendi, M. G. *J. Phys. Chem. B* **1997**, *101*, 9463. (b) Danek, M.; Jensen, K. F.; Murray, C. B.; Bawendi, M. G. *J. Cryst. Growth* **1994**, *145*, 714. (c) Danek, M.; Jensen, K. F.; Murray, C. B.; Bawendi, M. G. *Chem. Mater.* **1996**, *8*, 173. (d) Rodriguez-Viejo, J.; Jensen, K. F.; Mattoussi, H.; Michel, J.; Dabbousi, B. O.; Bawendi, M. G. *Appl. Phys. Lett.* **1997**, *70*, 2132. (e) Lee, J.; Sundar, V. C.; Heine, J. R.; Bawendi, M. G.; Jensen, K. F. *Adv. Mater.* **2000**, *12*, 1102.
(155) Micic, O. I.; Smith, B. B.; Nozik, A. J. *J. Phys. Chem. B* **2000**, *104*, 12149.
(156) Schreder, B.; Schmidt, T.; Ptatschek, V.; Winkler, U.; Materny, A.; Umbach, E.; Lerch, M.; Muller, G.; Kiefer, W.; Spanhel, L. *J. Phys. Chem. B* **2000**, *104*, 1677.
(157) Yang, C.-S.; Kauzlarich, S. M.; Wang, Y. C. *Chem. Mater.* **1999**, *11*, 3666.
(158) Brus, L. E. *Adv. Mater.* **1993**, *5*, 286.
(159) (a) Hasselbarth, A.; Eychmuller, A.; Eichberger, R.; Giersig, M.; Mews, A.; Weller, H. *J. Phys. Chem.* **1993**, *97*, 5333. (b) Mews, A.; Eychmuller, A.; Giersig, M.; Schooss, D.; Weller, H. *J. Phys. Chem.* **1994**, *98*, 934. (c) Mews, A.; Kadavanich, A. V.; Banin, U.; Alivisatos, A. P. *Phys. Rev. B* **1996**, *53*, R13242. (d) Mews,

A.; Eychmuller, A. *Ber. Bunsen-Ges. Phys. Chem.* **1998**, *102*, 1343. (e) Harrison, M. T.; Kershaw, S. V.; Rogach, A. L.; Kornowski, A.; Eychmüller, A.; Weller, H. *Adv. Mater.* **2000**, *12*, 123.
(160) (a) Zhou, H. S.; Honma, I.; Komiyama, H.; Haus, J. W. *J. Phys. Chem.* **1993**, *97*, 895. (b) Zhou, H. S.; Sasahara, H.; Honma, I.; Komiyama, H.; Haus, J. W. *Chem. Mater.* **1994**, *6*, 1534.
(161) (a) Gorer, S.; Ganske, J. A.; Hemminger, J. C.; Penner, R. M. *J. Am. Chem. Soc.* **1998**, *120*, 9584. (b) Gorer, S.; Penner, R. M. *J. Phys. Chem. B* **1999**, *103*, 5750.
(162) Elder, S. H.; Cot, F. M.; Su, Y.; Heald, S.; Tyryshkin, A. M.; Bowman, M. K.; Gao, Y.; Joly, A. G.; Balmer, M. L.; Kolwaite, A. C.; Magrini, K. A.; Blake, D. M. *J. Am. Chem. Soc.* **2000**, *122*, 5138.
(163) (a) Wang, Y.; Herron, N. *Chem. Phys. Lett.* **1992**, *200*, 71. (b) Wang, Y.; Herron, N. *J. Lumin.* **1996**, *70*, 48.
(164) Gallagher, D.; Heady, W. E.; Racz, J. M.; Bhargawa, R. N. *J. Cryst. Growth* **1994**, *138*, 970.
(165) (a) Colvin, V. L.; Schlamp, M. C.; Alivisatos, A. P. *Nature* **1994**, *370*, 354. (b) Gao, M.; Richter, B.; Kirstein, S.; Möhwald, H. *J. Phys. Chem. B* **1998**, *102*, 4096.
(166) Noglik, H.; Pietro, W. J. *Chem. Mater.* **1995**, *7*, 1333.
(167) Dabbousi, B. O.; Bawendi, M. G.; Onitsuka, O.; Rubner, M. F. *Appl. Phys. Lett.* **1995**, *66*, 1316.
(168) Sperling, V.; Woggon, U.; Lohde, A.; Haalboom, T. *J. Lumin.* **1997**, *72*, 395.
(169) (a) Greenham, N. C.; Peng, X.; Alivisatos, A. P. *Phys. Rev. B* **1996**, *54*, 17628. (b) Greenham, N. C.; Peng, X.; Alivisatos, A. P. *Synth. Met.* **1997**, 84, 545. (c) Ginger, D. S.; Greenham, N. C. *Synth. Met.* **1999**, *101*, 425.
(170) (a) Fogg, D. E.; Radzilowski, L. H.; Blanski, R.; Schrock, R. R.; Thomas, E. L. *Macromolecules* **1997**, *30*, 417. (b) Fogg, D. E.; Radzilowski, L. H.; Dabbousi, B. O.; Schrock, R. R.; Thomas, E. L.; Bawendi, M. G. *Macromolecules* **1997**, *30*, 8433.
(171) Schwerzel, R. E.; Spahr, K. B.; Kurmer, J. P.; Wood, V. E.; Jenkins, J. A. *J. Phys. Chem. A* **1998**, *102*, 5622.
(172) Li, S.; El-Shall, S. *Appl. Surf. Sci.* **1998**, *127*−*129*, 330.
(173) (a) Mattoussi, H.; Radzilowski, L. H.; Dabbousi, B. O.; Thomas, E. L.; Bawengi, M. G.; Rubner, M. F. *J. Appl. Phys.* **1998**, *83*, 7965. (b) Mattoussi, H.; Radzilowski, L. H.; Dabbousi, B. O.; Fogg, D. E.; Schrock, R. R.; Thomas, E. L.; Rubner, M. F.; Bawendi, M. G. *J. Appl. Phys.* **1999**, *86*, 4390.
(174) Yao, H.; Takada, Y.; Kitamara, N. *Langmuir* **1998**, *14*, 595.
(175) (a) Sooklal, K.; Hanus, L. H.; Ploehn, H. J.; Murphy, C. J. *Adv. Mater.* **1998**, *10*, 1083. (b) Huang, J.; Sooklal, K.; Murphy, C. J.; Ploehn, H. J. *Chem. Mater.* **1998**, *11*, 3595.
(176) Huynh, W. U.; Peng, X.; Alivisatos, A. P. *Adv. Mater.* **1999**, *11*, 923.
(177) Lifshitz, E.; Sirota, M.; Porteanu, H. *J. Cryst. Growth* **1999**, *196*, 126.
(178) Sun, L.; Fu, X.; Wang, M.; Liu, C.; Liao, C.; Yan, C. *J. Lumin.* **2000**, *87*−*89*, 538.
(179) Kezuka, T.; Konishi, M.; Isoke, T.; Senna, M. *J. Lumin.* **2000**, *87*−*89*, 418.
(180) (a) Gao, M.; Lesser, C.; Kirstein, S.; Möhwald, H.; Rogach, A.; Weller, H. *J. Appl. Phys.* **2000**, *87*, 2297. (b) Rogach, A. L.; Koktysh, D. S.; Harrison, M.; Kotov, N. A. *Chem. Mater.* **2000**, *12*, 1526. (c) Gaponik, N. P.; Talapin, D. V.; Rogach, A. L.; Eychmüller, A. *J. Mater. Chem.* **2000**, *10*, 2163.
(181) Huang, J. M.; Yang, Y.; Yang, B.; Liu, S. Y.; Shen, J. C. *Thin Solid Films* **1998**, *327*−*329*, 536.
(182) Mastai, Y.; Gal, D.; Hodes, G. *J. Electrochem. Soc.* **2000**, *147*, 1435.
(183) Torimoto, T.; Obayashi, A.; Kuwabata, S.; Yoneyama, H. *Electrochem. Commun.* **2000**, *2*, 359.
(184) Gerischer, H.; Lubke, M. *J. Electroanal. Chem.* **1986**, *204*, 225.
(185) (a) Spanhel, L.; Weller, H.; Henglein, A. *J. Am. Chem. Soc.* **1987**, *109*, 6632. (b) Vogel, R.; Hoyer, P.; Weller, H. *Chem. Phys. Lett.* **1990**, *174*, 241.
(186) Gopidas, K. R.; Bohorquez, M.; Kamat, P. V. *J. Phys. Chem.* **1990**, *94*, 6435.
(187) (a) Fujii, H.; Ohtaki, M.; Eguchi, K.; Arai, H. *J. Mol. Catal. A: Chem.* **1998**, *129*, 61. (b) Fujii, H.; Ohtaki, M.; Eguchi, K.; Arai, H. *J. Appl. Electrochem.* **1997**, 1086.
(188) Serpone, N.; Borgarello, E.; Gratzel, M. *J. Chem. Soc., Chem. Commun.* **1983**, 342.
(189) Hotchandani, S.; Kamat, P. V. *J. Phys. Chem.* **1992**, *96*, 6834.
(190) (a) Spanhel, L.; Henglein, A.; Weller, H. *Ber. Bunsen-Ges. Phys. Chem.* **1987**, *91*, 1359. (b) Henglein, A.; Guitierrez, M.; Weller, H.; Fojtik, A.; Jirkovsky, J. *Ber. Bunsen-Ges. Phys. Chem.* **1989**, *93*, 593. (c) Spanhel, L.; Weller, H.; Fojtik, A.; Henglein, A. *Ber. Bunsen-Ges. Phys. Chem.* **1987**, *91*, 88.
(191) Sun, Y.; Hao, E.; Zhang, X.; Yang, B.; Gao, M.; Shen, J. *J. Chem. Soc., Chem. Commun.* **1996**, 2381.
(192) Di Paola, A.; Palmisano, L.; Venezia, A. M.; Augugliaro, V. *J. Phys. Chem. B* **1999**, *103*, 8236.
(193) Rabani, J. *J. Phys. Chem.* **1992**, *96*, 7707.
(194) Kamat, P. V.; Patrik, P. *J. Phys. Chem.* **1992**, *96*, 6829.
(195) Hao, E.; Sun, H.; Zhou, Z.; Liu, J.; Yang, B.; Shen, J. *Chem. Mater.* **1999**, *11*, 3096.
(196) (a) Kakuta, N.; Park, K. H.; Finlayson, M. F.; Ueno, A.; Bard, A. J.; Campion, A.; Fox, M. A.; Webber, S. E.; White, J. M. *J. Phys. Chem.* **1985**, *89*, 732. (b) Ueno, A.; Kakuta, N.; Park, K. H.; Finlayson, M. F.; Bard, A. J.; Campion, A.; Fox, M. A.; Webber, S. E.; White, J. M. *J. Phys. Chem.* **1985**, *89*, 3828.
(197) Chenthamarakshan, C. R.; Ming, Y.; Rajeshwar, K. *Chem. Mater.* **2000**, *12*, 3538.
(198) Beydoun, D.; Amal, R.; Low, G. K.-C.; McEvoy, S. *J. Phys. Chem. B* **2000**, *104*, 4387.
(199) Uekawa, N.; Suzuki, T.; Ozeki, S.; Kaneko, K. *Langmuir* **1992**, *8*, 1.
(200) Shiyanovskaya, I.; Hepel, M. *J. Electrochem. Soc.* **1999**, *146*, 243.
(201) Ocana, M.; Hsu, W. P.; Matijevic, E. *Langmuir* **1991**, *7*, 2911.
(202) Kamat, P. V. In *Molecular Level Artificial Photosynthetic Materials*; Meyer, G. J., Ed.; Wiley: New York, 1997; pp 273−343.
(203) Dawson, A.; Kamat, P. V. *J. Phys. Chem. B* **2000**, *105*, 960.
(204) (a) Deguchi, T.; Imai, K.; Iwasaki, M.; Tada, H.; Ito, S. *J. Electrochem. Soc.* **2000**, *147*, 2263. (b) Tada, H.; Teranishi, K.; Inubushi, Y.; Ito, S. *Langmuir* **2000**, *16*, 3304.
(205) Matsumura, M.; Ohno, T.; Saito, S.; Ochi, M. *Chem. Mater.* **1996**, *8*, 1370.
(206) (a) Sadeghi, M.; Liu, W.; Zhang, T.-G.; Stavropoulos, P.; Levy, B. *J. Phys. Chem.* **1996**, *100*, 19466. (b) Haick, H.; Paz, Y. *J. Phys. Chem. B* **2001**, *105*, 3045.
(207) (a) Nozik, A. J. *Appl. Phys. Lett.* **1976**, *29*, 150. (b) Fornarini, L.; Nozik, A. J.; Parkinson, B. A. *J. Phys. Chem.* **1984**, *88*, 3238.
(208) Yuan, J.; Tsujikawn, S. *J. Electrochem. Soc.* **1995**, *142*, 3444.
(209) Nosaka, Y.; Norimatsu, K.; Miyama, H. *Chem. Phys. Lett.* **1984**, *106*, 128.
(210) Aspnes, D. E.; Heller, A. *J. Phys. Chem.* **1983**, *87*, 4919.
(211) (a) Nakato, Y.; Abe, K.; Tsubomura, H. *Ber Bunsen-Ges. Phys. Chem.* **1976,** *80*, 1002. (b) Nakato, Y.; Shioji, M.; Tsubomura, H. *Chem. Phys. Lett.* **1982**, *90*, 453. (c) Nakato, Y.; Ueda, K.; Tsubomura, H. *J. Phys. Chem.* **1986**, *90*, 5495.
(212) Hiesgen, R.; Meissner, D. *J. Phys. Chem. B* **1998**, *102*, 6549.
(213) Nemanick, E. J.; Rossi, R. C.; Lewis, N. S. In 13th International Conference on Photochemical Conversion and Storage of Solar Energy (IPS 2000), July 30−August 4, Snowmass, CO, 2000; paper no. W7-p-14.
(214) Rajeshwar, K. *J. Appl. Electrochem.* **1985**, *15*, 1.
(215) Fox, M. A.; Dulay, M. T. *Chem. Rev.* **1993**, *93*, 341.
(216) Hoffman, M. R.; Martin, S. T.; Choi, W.; Bahnemann, D. W. *Chem. Rev.* **1995**, *95*, 69.
(217) (a) Weller, H. *Ber. Bunsen-Ges. Phys. Chem.* **1991**, *95*, 1361. (b) Vogel, P.; Hoyer, P.; Weller, H. *J. Phys. Chem.* **1994**, *98*, 3183.
(218) (a) O'Regan, B.; Gratzel, M. *Nature* **1991**, *353*, 737. (b) Bach, U.; Lupo, D.; Comte, P.; Moser, J. E.; Weissortel, F.; Salbeck, J.; Spreitzer, H.; Gratzel, M. *Nature* **1998**, *395*, 583.
(219) (a) Tennekone, K.; Kumara, G. R. R. A.; Kottegoda, I. R. M.; Perera, V. P. S. *Chem. Commun.* **1999**, 15. (b) Tennakone, K.; Senadeera, G. K. R.; Perera, V. P. S.; Kottegoda, I. R. M.; De Silva, L. A. A. *Chem. Mater.* **1999**, *11*, 2474.
(220) Marks, R. N.; Halls, J. J. M.; Bradley, D. D. C.; Friend, R. H.; Holmes, A. B. *J. Phys. Condens. Matter* **1994**, *6*, 1379.
(221) Yu, G.; Zhang, C.; Heeger, A. J. *Appl. Phys. Lett.* **1994**, *64*, 1540.
(222) Peng, X.; Manna, L.; Yang, W.; Wickham, J.; Scher, E.; Kadavanich, A.; Alivisatos, A. P. *Nature* **2000**, *404*, 59.
(223) Guo, X.-C.; Dong, P. *Langmuir* **1999**, *15*, 5535.
(224) Jiang, P.; Bertone, J. F.; Colvin, V. L. *Science* **2001**, *291*, 453.
(225) Murray, C. B.; Kagan, C. R.; Bawendi, M. G. *Science* **1995**, *270*, 1335.
(226) (a) Nyffenegger, R. M.; Craft, B.; Shaaban, M.; Gorer, S.; Penner, R. M. *Chem. Mater.* **1998**, *10*, 1120. (b) Gorer, S.; Ganske, J. A.; Hemminger, J. C.; Penner, R. M. *J. Am. Chem. Soc.* **1998**, *120*, 9584. (c) Erley, G.; Gorer, S.; Penner, R. M. *Appl. Phys. Lett.* **1998**, *72*, 2301.
(227) Sopajaree, K.; Qasim, S. A.; Basak, S.; Rajeshwar, K. *J. Appl. Electrochem.* **1999**, *29*, 533.
(228) Ziolkowski, L.; Vinodgopal, K.; Kamat, P. V. *Langmuir* **1997**, *13*, 3124.
(229) Ohko, Y.; Saitoh, S.; Tatsuma, T.; Fujishima, A. *J. Electrochem. Soc.* **2001**, *148*, B24.
(230) Kim, H.; Hara, N.; Sugimoto, K. *J. Electrochem. Soc.* **1999**, *146*, 955.
(231) For example: Corrigan, D. A.; Knight, S. L. *J. Electrochem. Soc.* **1989**, *136*, 613.
(232) Bianconi, P. A.; Lin, J.; Strzelecki, A. R. *Nature* **1991**, *349*, 315.
(233) (a) Belcher, A. M., personal communication, 2001. (b) Whaley, S. R.; English, D. S.; Hu, E. L.; Barbara, P. F.; Belcher, A. M. *Nature* **2000**, *405*, 665.
(234) Chen, W. C. W.; Nie, S. *Science* **1998**, *281*, 2016.

CM010254Z